

QPS Confinement and Transport

Don Spong¹, L. Berry¹, S. Hirshman¹, J. Lyon¹,
D. Mikkelsen²,

¹Oak Ridge National Laboratory

²Princeton Plasma Physics Laboratory

13th INTERNATIONAL STELLARATOR WORKSHOP
Australian National University
Canberra, Australia



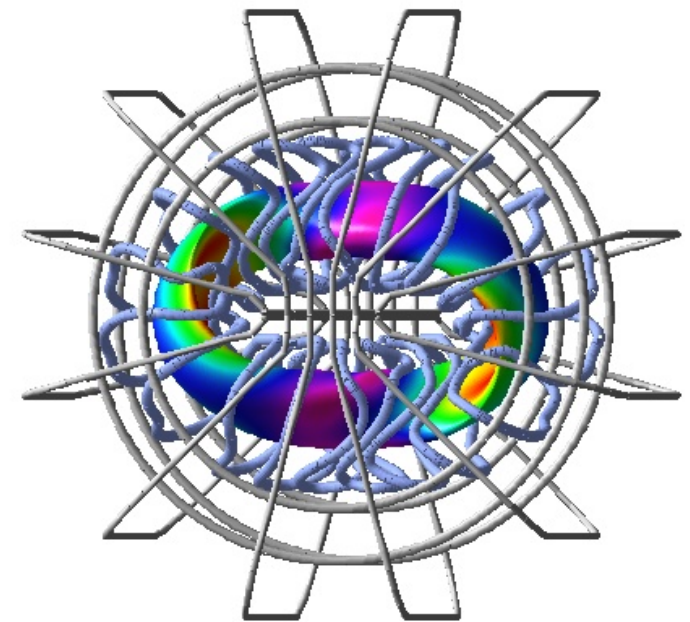
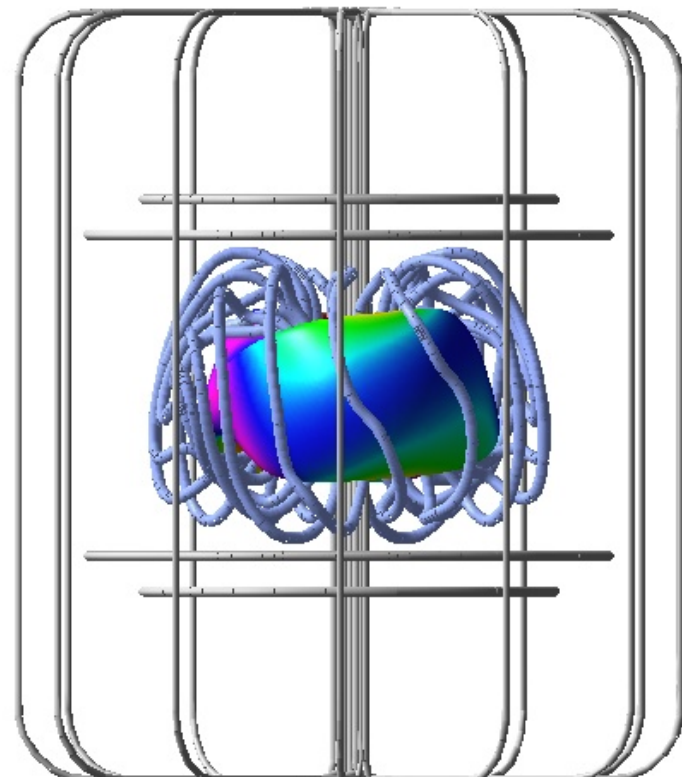
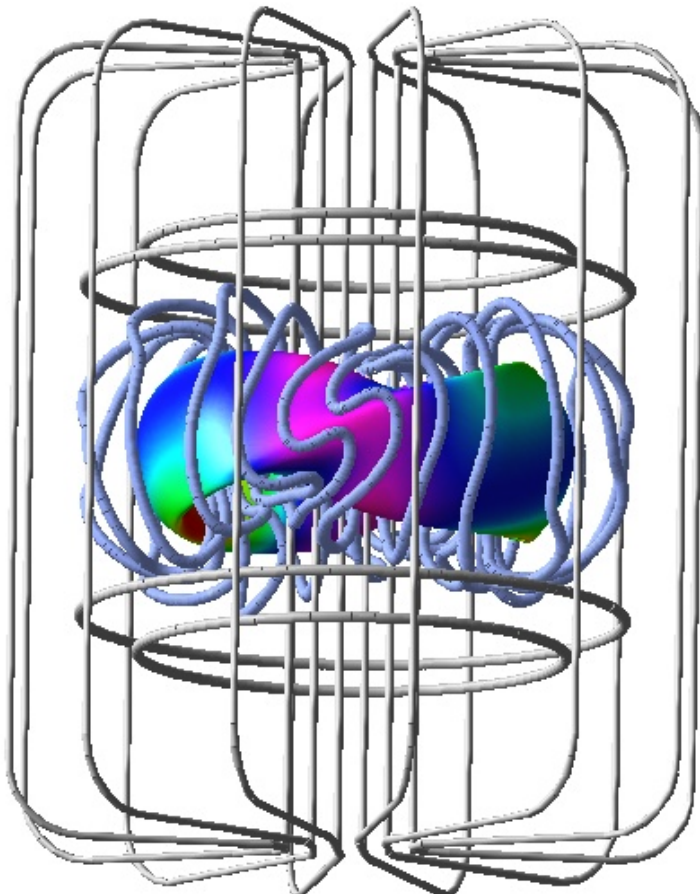
OAK RIDGE NATIONAL LABORATORY
U. S. DEPARTMENT OF ENERGY



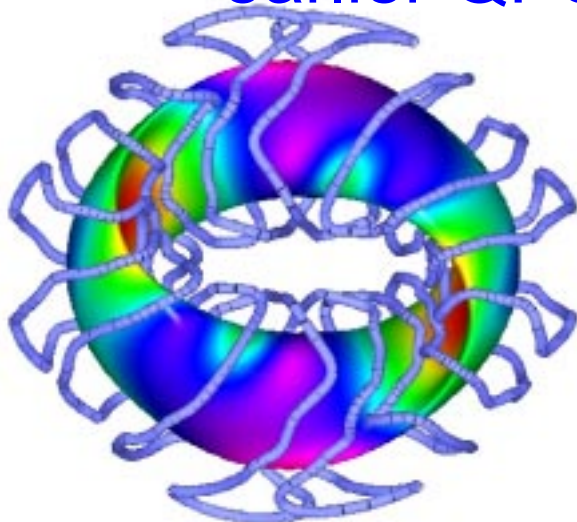
QPS Confinement and Transport Topics

- Is neoclassical stellarator transport sufficiently subdominant to anomalous transport ($\tau_{\text{neo}} \gg \tau_{\text{ISS95}}$)?
 - to allow well defined enhanced confinement regimes
 - we consider both low (ECH) and high collisionality (ICH) regimes
- Status of transport tools and QPS predictions
 - simple transport targets used in optimization
 - local diffusive transport models
 - DKES, NEO, 0-D, 1-D calculations
 - global Monte Carlo model
- Bootstrap current levels
 - To what extent do collisional/electric field effects modify bootstrap current?
 - Required incremental Ohmic currents
- Can significant β 's be attained?
 - to test bootstrap current/equilibrium robustness
 - to test stability

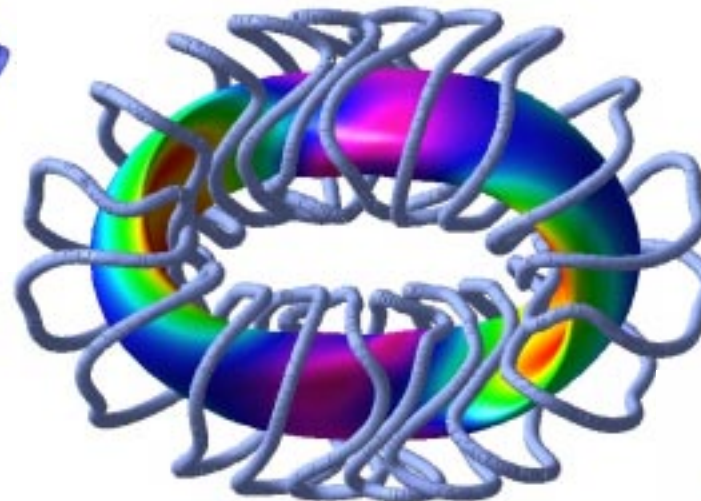
View of recent QPS
configuration with modular,
vertical and toroidal field coils:



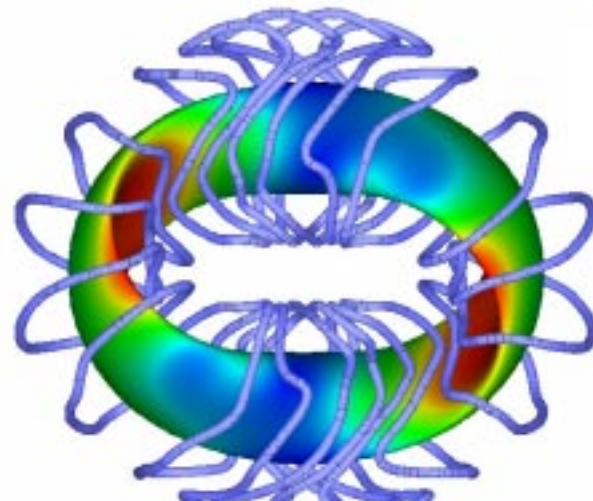
The QPS design has been evolving : several earlier QPS configurations are analyzed here



GB4 - PVR Ref.

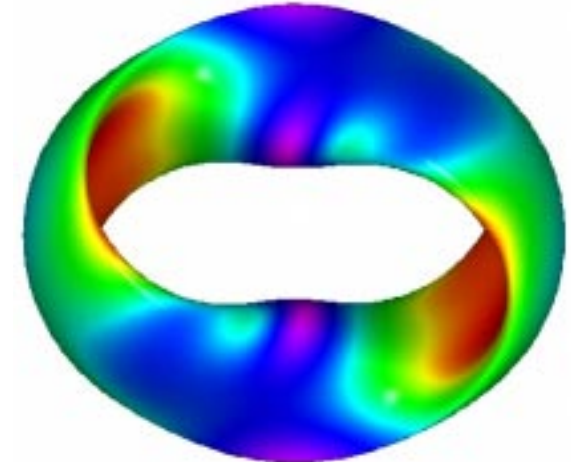


Current
1108a4

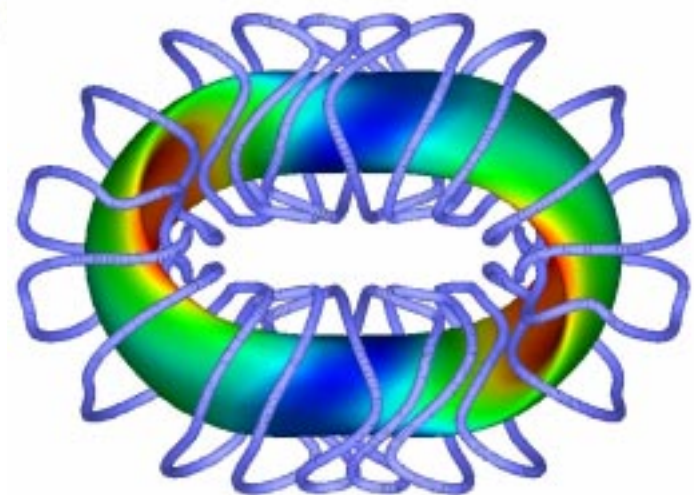


QPS 080301

(similar to 926, 929)



GB5



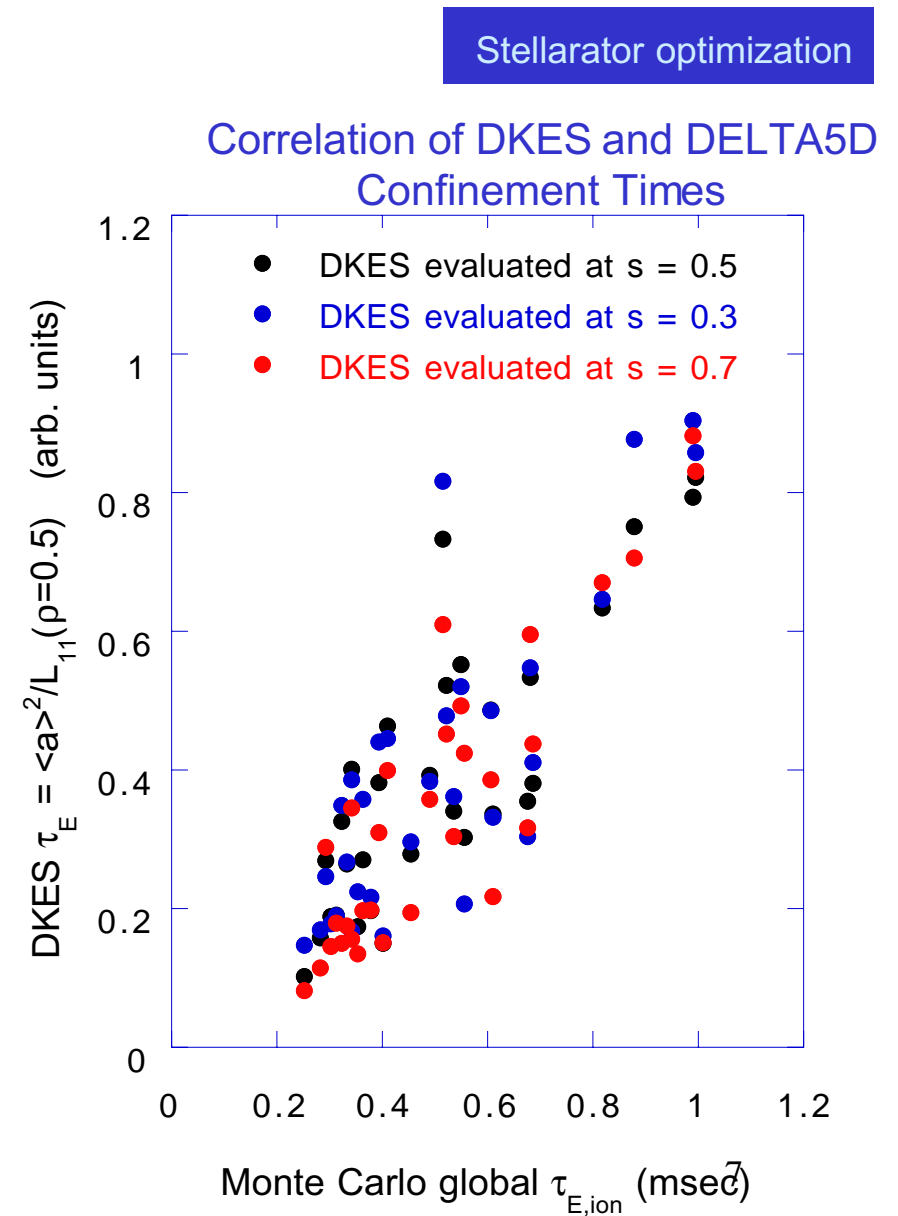
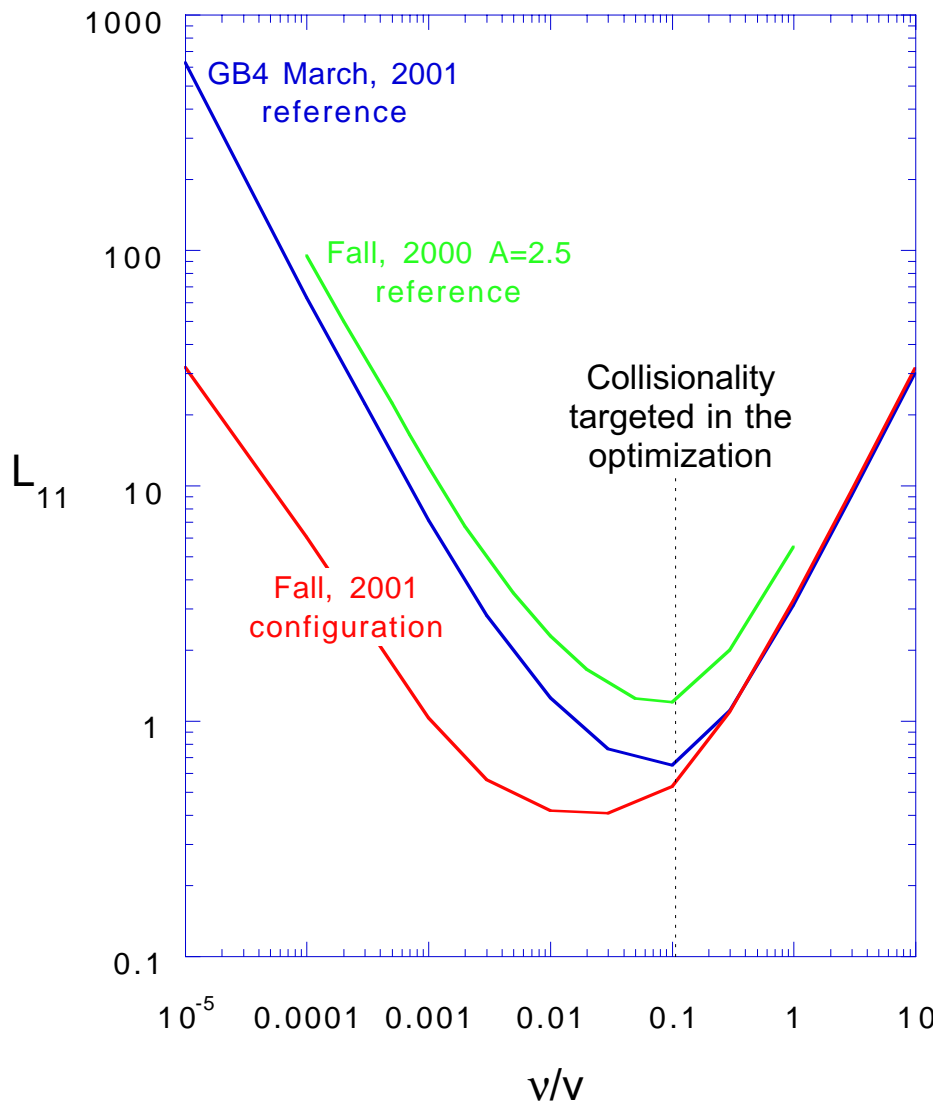
QPS 1016 ⁴

QPS TRANSPORT OPTIMIZATION

Transport Tools used to Evaluate QPS configurations:

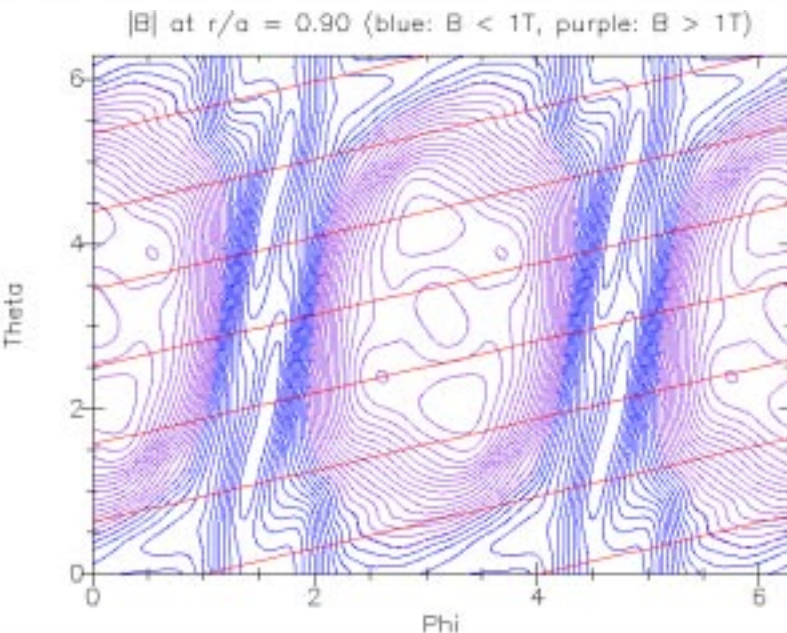
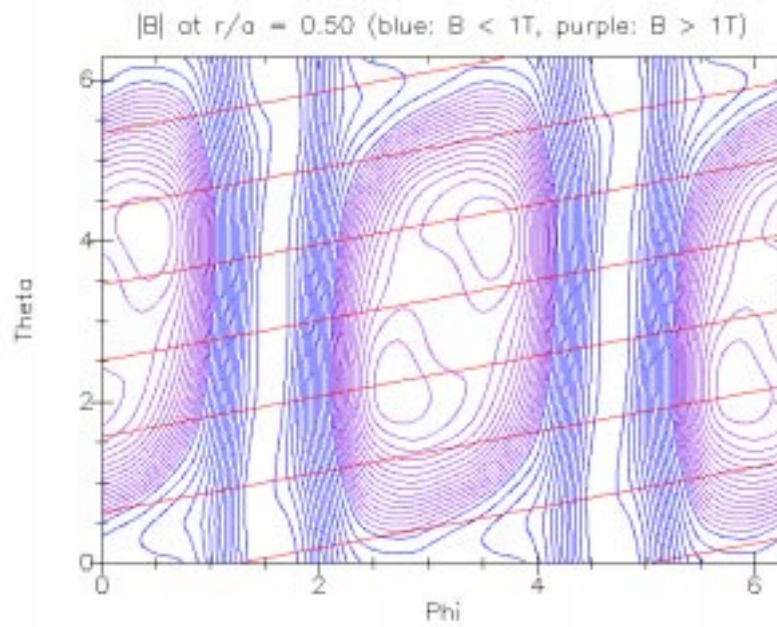
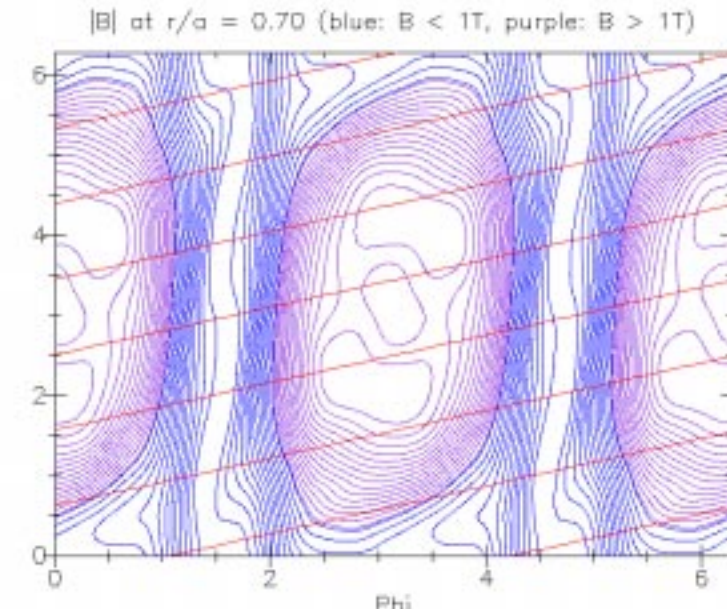
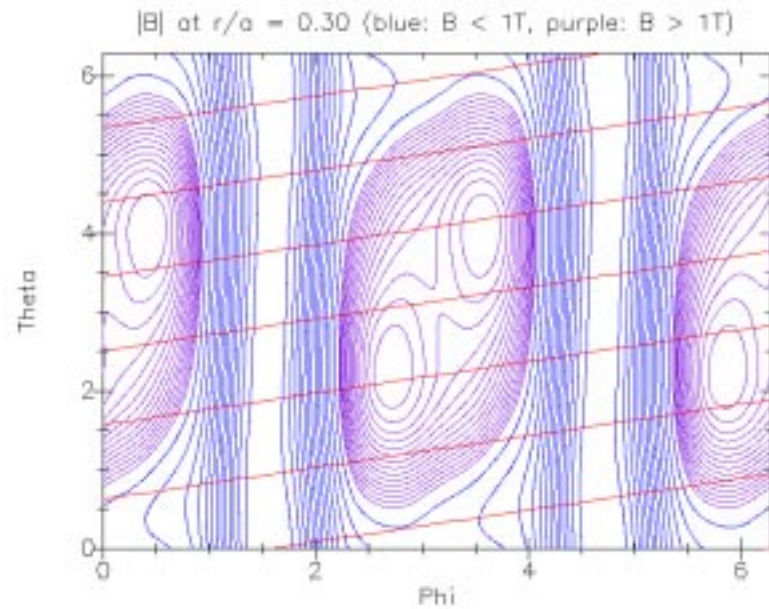
Transport tool	Physical Model	Fixed Parameters	Predicted Parameters
0-D model	ISS95	P_{heat} , n	β , τ_E , T
1-D model	ISS95 + Simplified neoclassical	$P_{heat}(r)$, $n(r)$	$T(r)$, τ_E , $P_{loss}(r)$
NEO	$1/v$, $E_r = 0$ neoclassical	n' , T'	$\epsilon_{eff}^{3/2}$
DKES	Local neoclassical	n' , T' , E_r , v	Transport coefficient matrix
Monte Carlo	Large orbit global neoclassical	$N(r)$, $T(r)$, $\phi(r)$	τ_E , τ_p , ϕ_0

Transport optimizations using the NEO/DKES transport targets have resulted in confinement improvement.

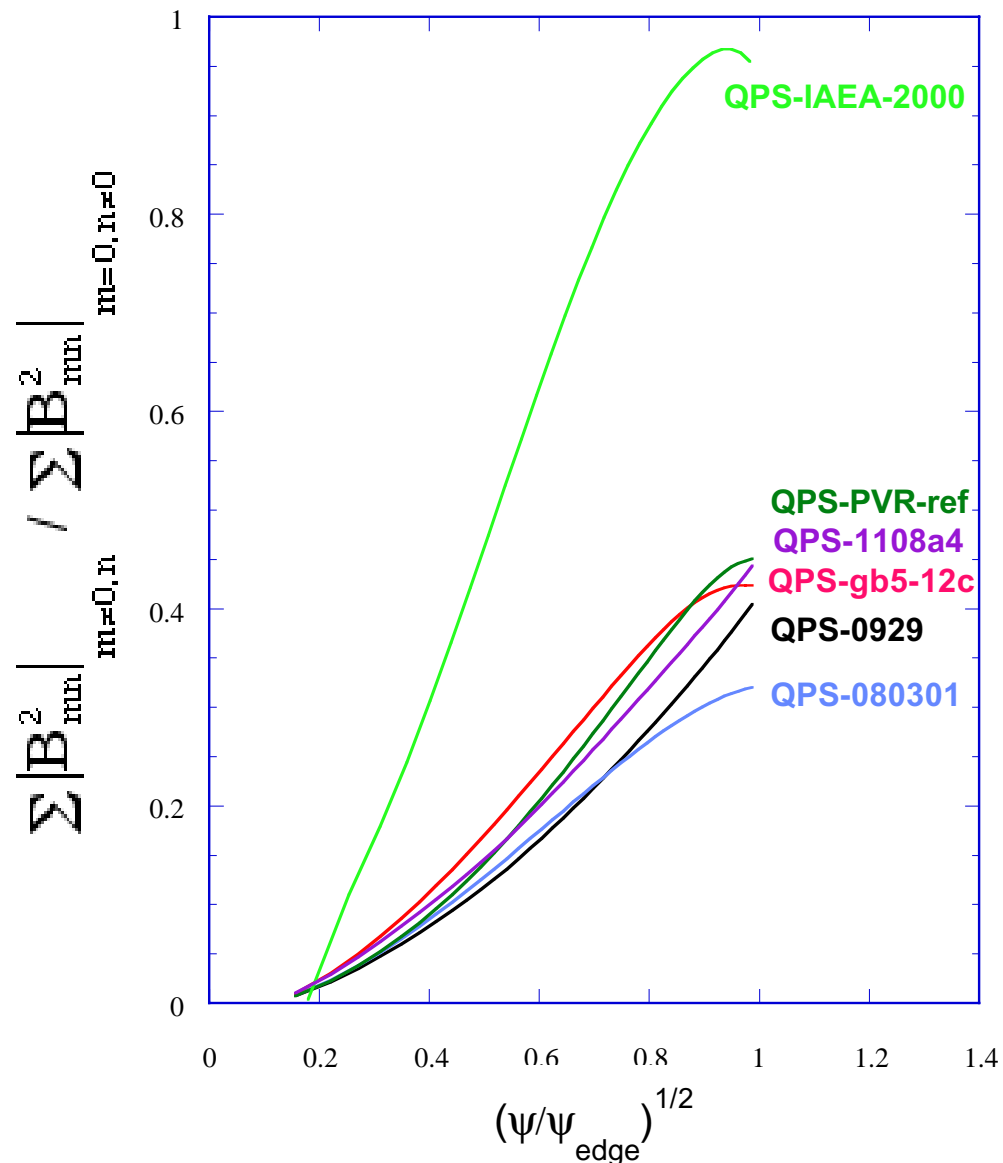


QPS MAGNETIC STRUCTURE

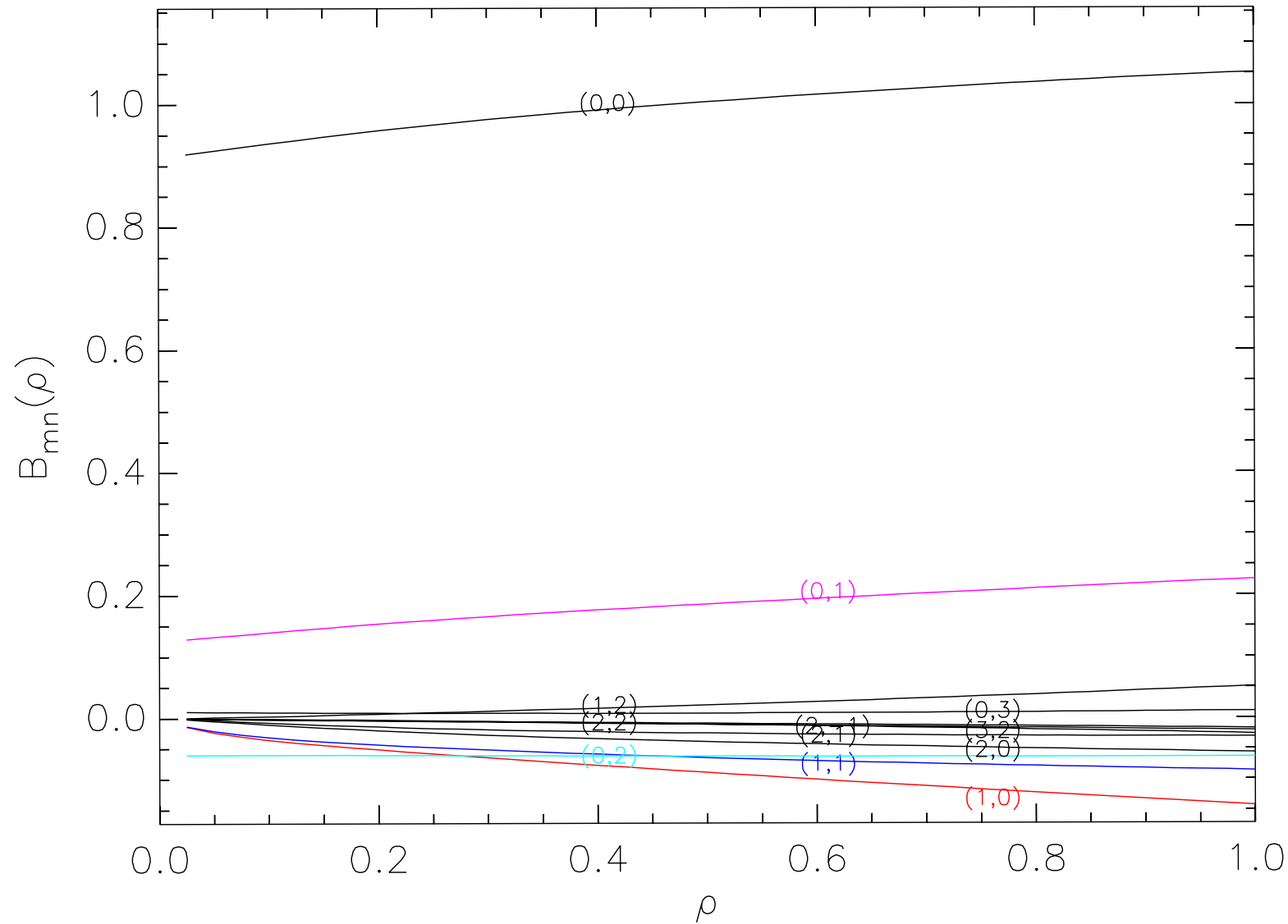
The variation of $|B|$ on flux surfaces at “ r/a ” = 0.3, 0.5, 0.7, 0.9 shows the quasi-poloidal symmetry about which QPS devices have been optimized:



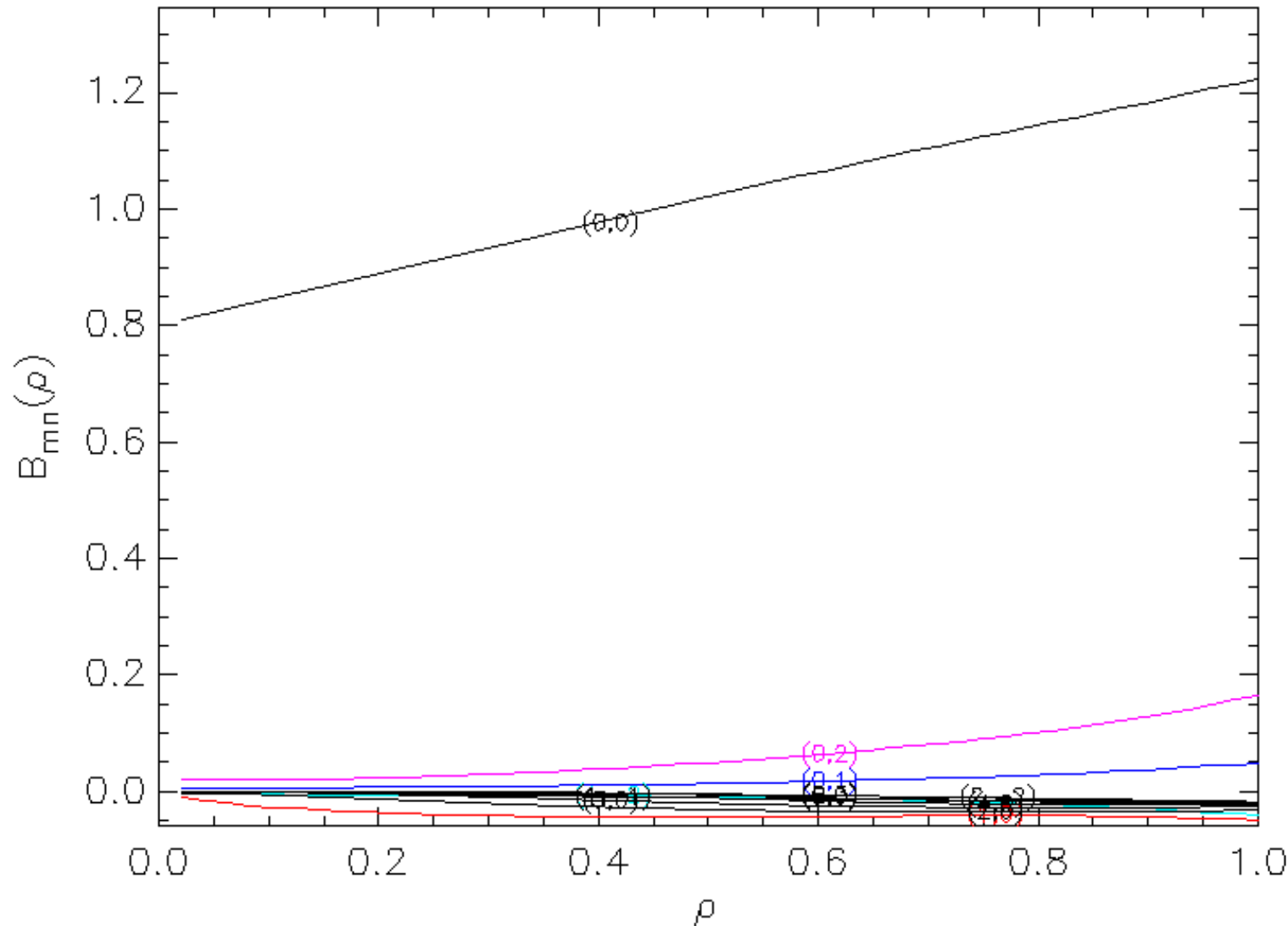
The ratio of magnetic energy in non-poloidally symmetric modes to the magnetic energy in poloidally symmetric modes (excluding $m = n = 0$) is used as a measure of quasi-poloidal symmetry.



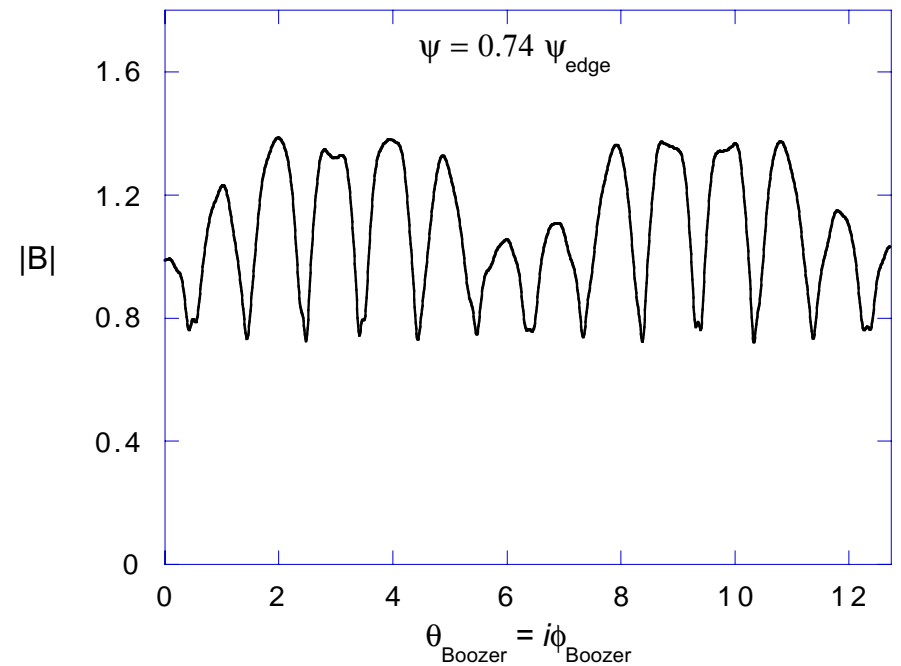
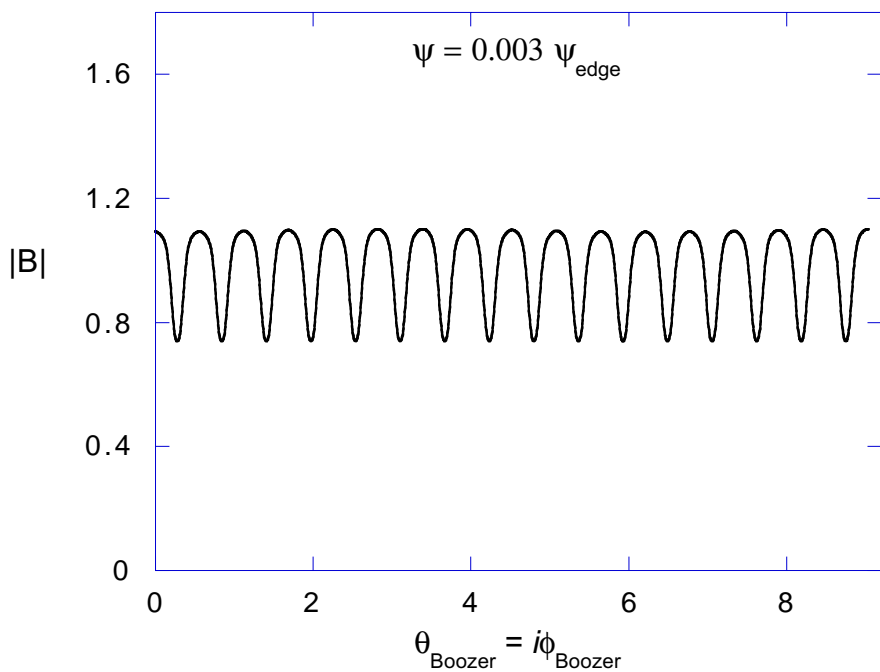
The B_{mn} spectrum for the QPS 1108a4 device shows that the dominant symmetry is in the poloidal direction



At high β 's (= 15% here) the QPS B_{mn} spectrum becomes increasingly quasi-poloidal.



Variation of $|B|$ along a field line for QPS_1016 configuration (near axis and edge): Minima are well aligned leading to good trapped particle confinement



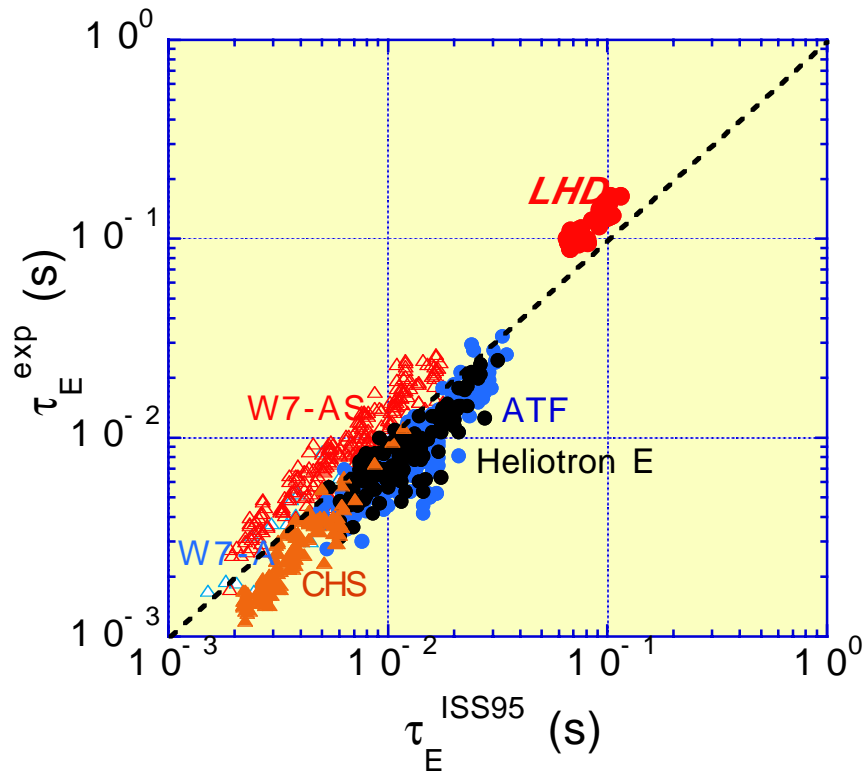
QPS O-D AND 1-D TRANSPORT ANALYSIS

Global stellarator confinement scalings

$$\tau_E^{\text{ISS95}} = 0.079 H_{\text{ISS95}} a_p^{2.21} R^{0.65} P^{-0.59} n^{0.51} B^{0.83} \iota^{-0.4}$$

$$\tau_E^{\text{ISS95}} = W_{\text{tot}} / P \quad W_{\text{tot}} = 1.5 \langle \beta \rangle (B_0^2 / 2\mu_0) V_p \quad \text{0-D model}$$

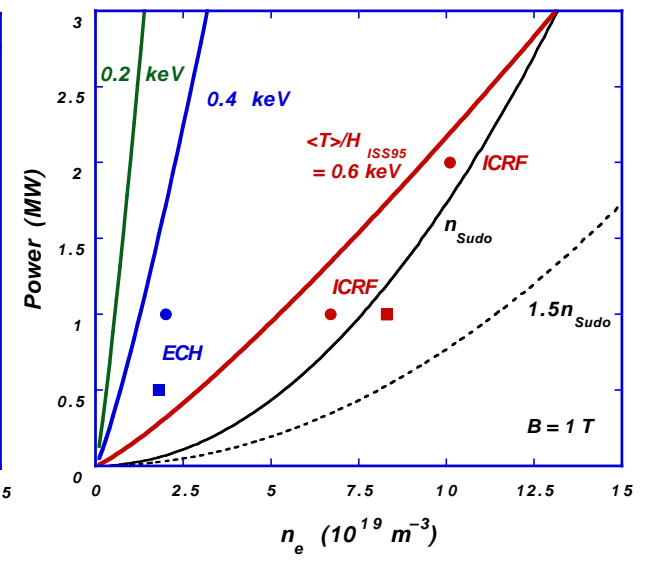
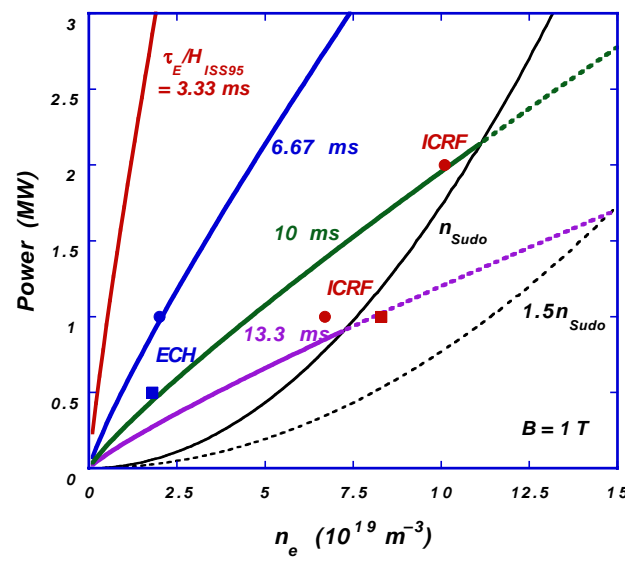
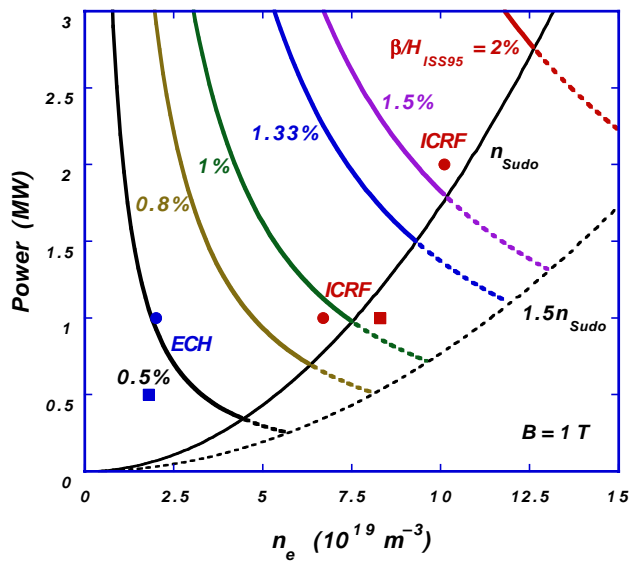
$$n_{\text{Sudo}} = 0.25 [P/B / R a_p^2]^{1/2}$$



- Data only for $R/a_p > 5$
- W7-AS and LHD find H_{ISS95} up to 2.5
 - low shear, large a_p
- For fixed a_p, R, n, B, ι , can calculate:
 - $\langle T \rangle / H_{\text{ISS95}}$
 - $\langle \beta \rangle / H_{\text{ISS95}}$
 - $\tau_E / H_{\text{ISS95}}$

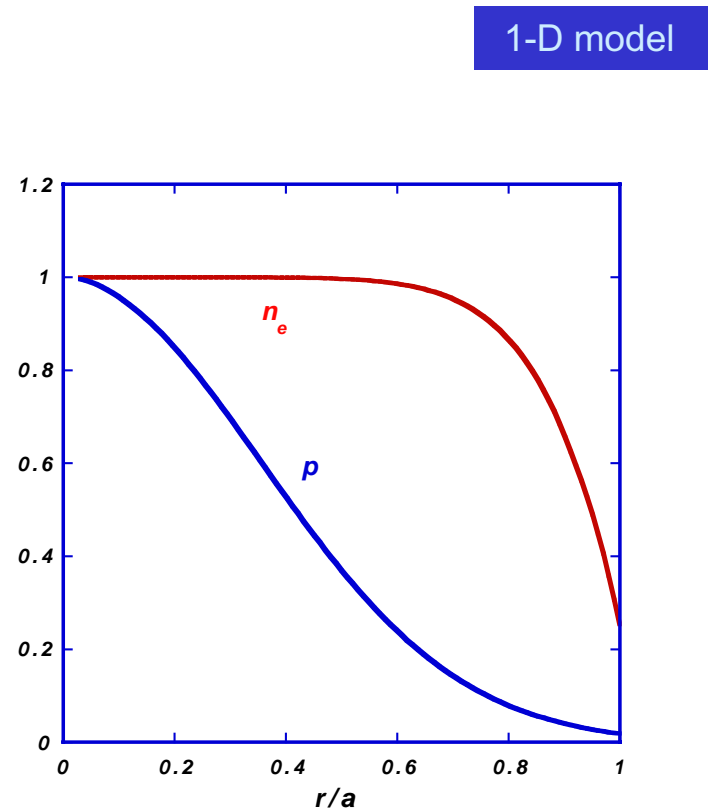
Global stellarator confinement scalings indicate the QPS CE device can achieve adequate plasma performance for its mission

0-D model



1-D Model (Dave Mikkelsen) includes profile effects and self-consistent ambipolar electric field

- Coupled electrons/ion power balance equations
- Ambipolar particle balance for helical ripple component
- Thermal diffusivities
 - Neoclassical ripple coefficient using $\varepsilon_{\text{eff}}^{3/2}$ from NEO code
 - E_r dependence from Shaing-Houlberg single helicity model
- Density and power deposition profiles assumed as shown

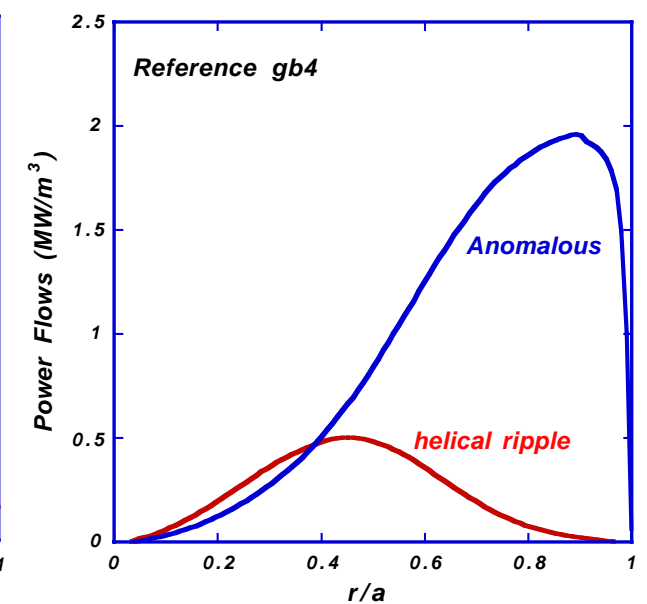
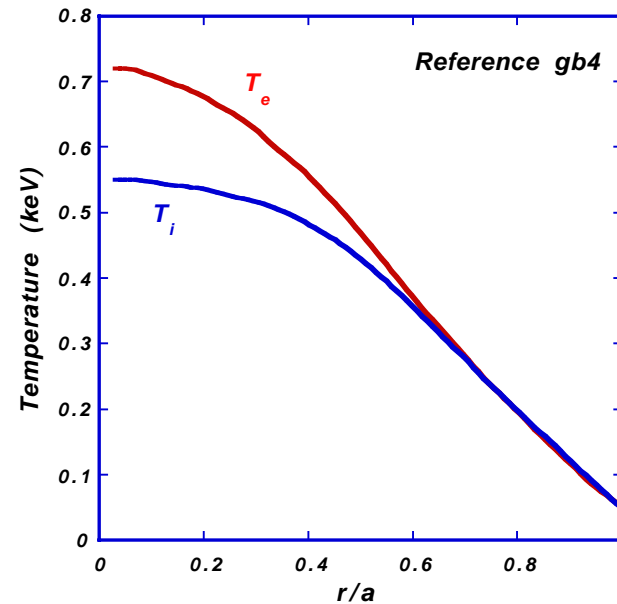
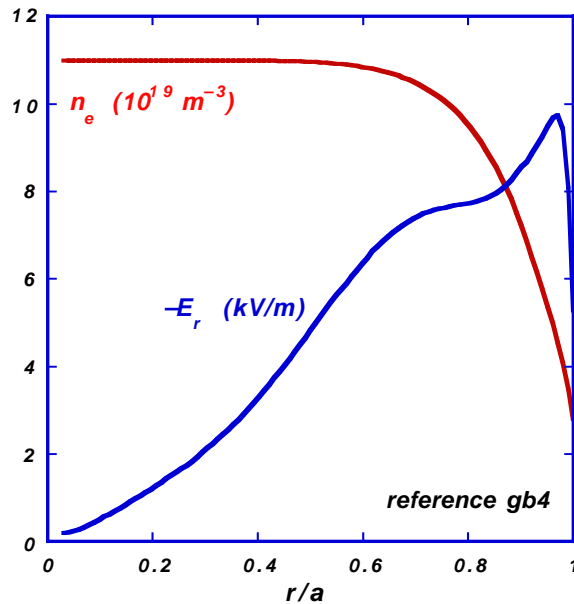


This model has been motivated by more comprehensive calculations (DKES, Monte Carlo)

ICRF Heated plasmas

Device	τ_E (msec)	$\langle \beta \rangle$	1-D model
gb4	18.3	1.4	
gb5_12c	18.8	1.44	
gb5_12d	18.9	1.46	

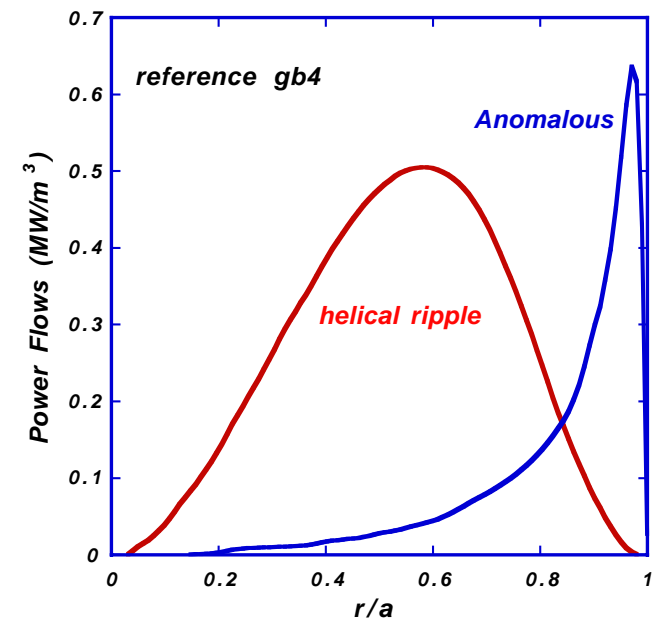
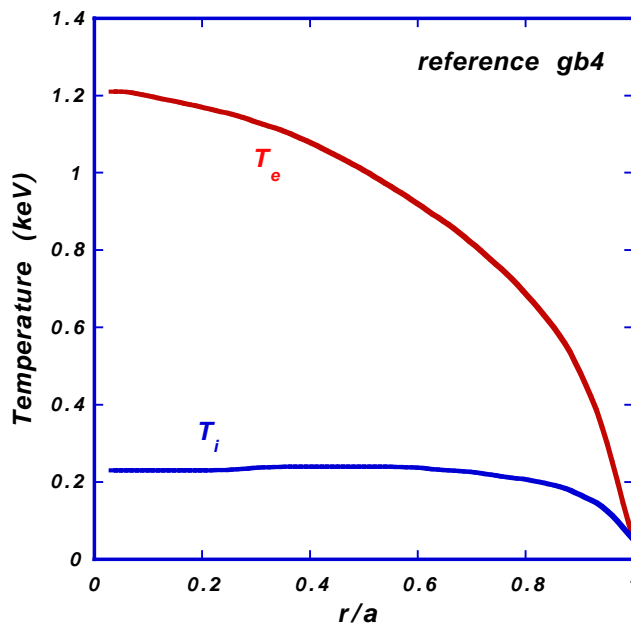
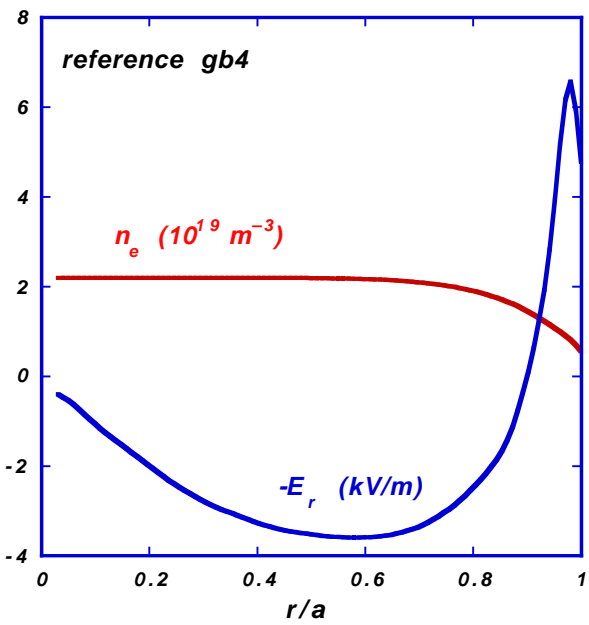
For $B = 1\text{T}$, $P_{\text{ICRF}} = 1\text{Mw}$



ECRF Heated plasmas - gb4 configuration

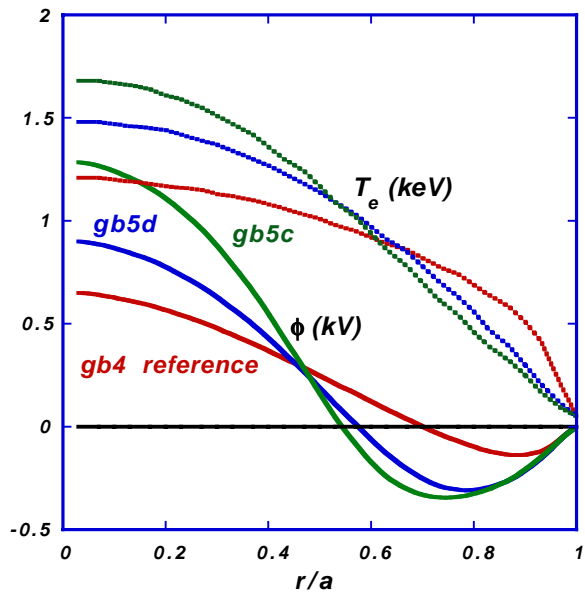
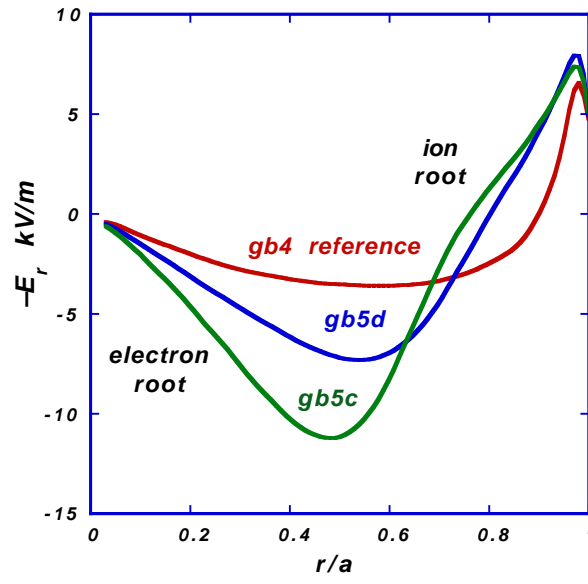
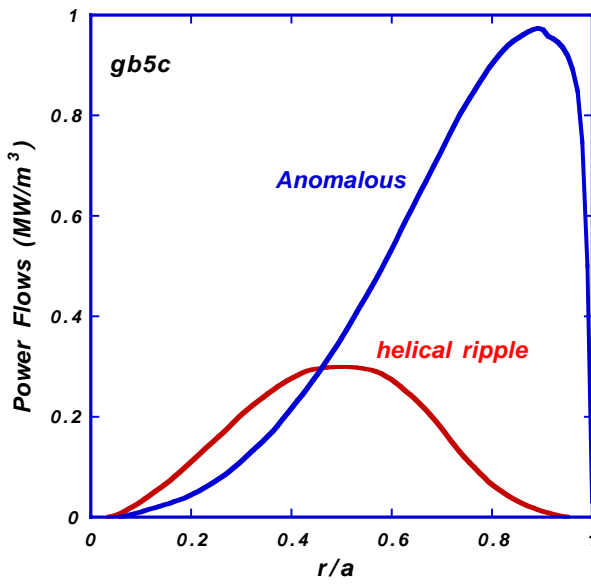
Device	$\tau_E(\text{msec})$	$\langle \beta \rangle$	1-D model
gb4	10.0	0.77	

For $B = 1\text{T}$, $P_{\text{ECRF}} = 1\text{Mw}$



ECRF Heated gb5 configuration has helical ripple component that is subdominant to anomalous

Device	$\tau_E(\text{msec})$	$\langle \beta \rangle$	1-D model
gb4	10.0	0.77	
gb5c	10.1	0.78	
gb5d	10.2	0.79	



QPS DKES AND NEO TRANSPORT ANALYSIS

The DKES (Drift Kinetic Equation Solver) provides the full neoclassical transport coefficient matrix (multi-helicity)

DKES Transport analysis

$$I_i = \begin{bmatrix} \vec{\Gamma} \bullet \vec{\nabla}_S \\ \frac{1}{T} \vec{Q} \bullet \vec{\nabla}_S \\ n \langle (\vec{u} - \vec{u}_s) \bullet \vec{B} \rangle \end{bmatrix} = -\sum_{j=1}^3 D_{ij} A_j \quad A_j = \begin{bmatrix} \frac{n'}{n} - \frac{3}{2} \frac{T'}{T} - \frac{eE_r}{T} \\ \frac{T'}{T} \\ -\left(\frac{e}{T}\right) \left(\frac{\langle \vec{E} \bullet \vec{B} \rangle}{\langle B^2 \rangle} \right) \end{bmatrix}$$

$$D_{ij} = n \frac{2}{\sqrt{\pi}} \int_0^\infty dK \sqrt{K} e^{-K} g_i g_j D_{ij}$$

$$\text{where } g_1 = g_3 = 1, \quad g_2 = K, \quad K = \left(\frac{v}{v_{th}} \right)^2$$

$$D_{11} = D_{12} = D_{21} = D_{22} = -\frac{v_{th}}{2} \left[\frac{B v_{th}}{\Omega} \left(\frac{d\rho}{dr} \right)^{-1} \right]^2 K \sqrt{K} L_{11}$$

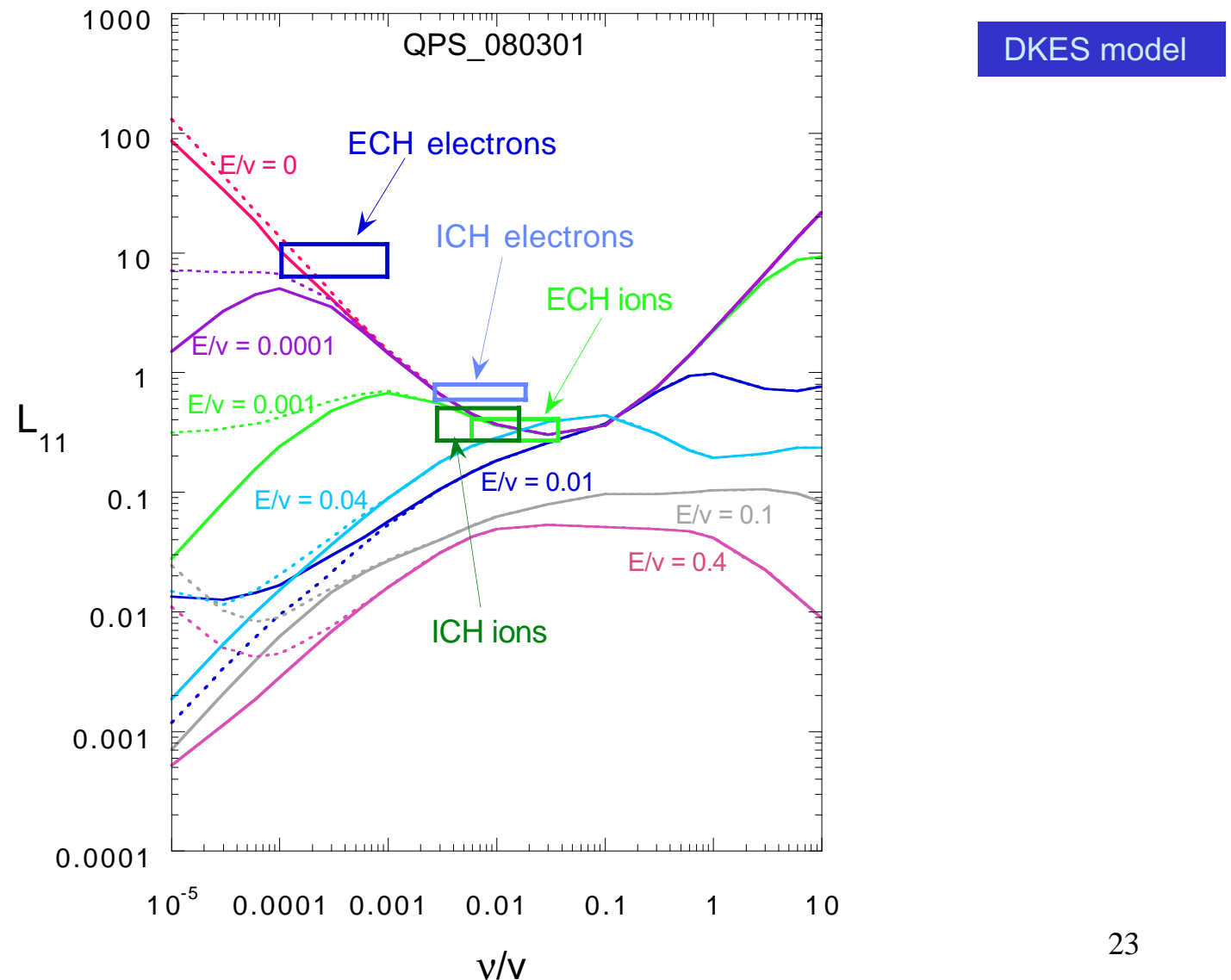
$$D_{31} = D_{32} = -D_{13} = -D_{23} = -\frac{v_{th}}{2} \left[\frac{B v_{th}}{\Omega} \left(\frac{d\rho}{dr} \right)^{-1} \right] K L_{31}$$

$$D_{33} = -\frac{v_{th}}{2} \sqrt{K} L_{33}$$

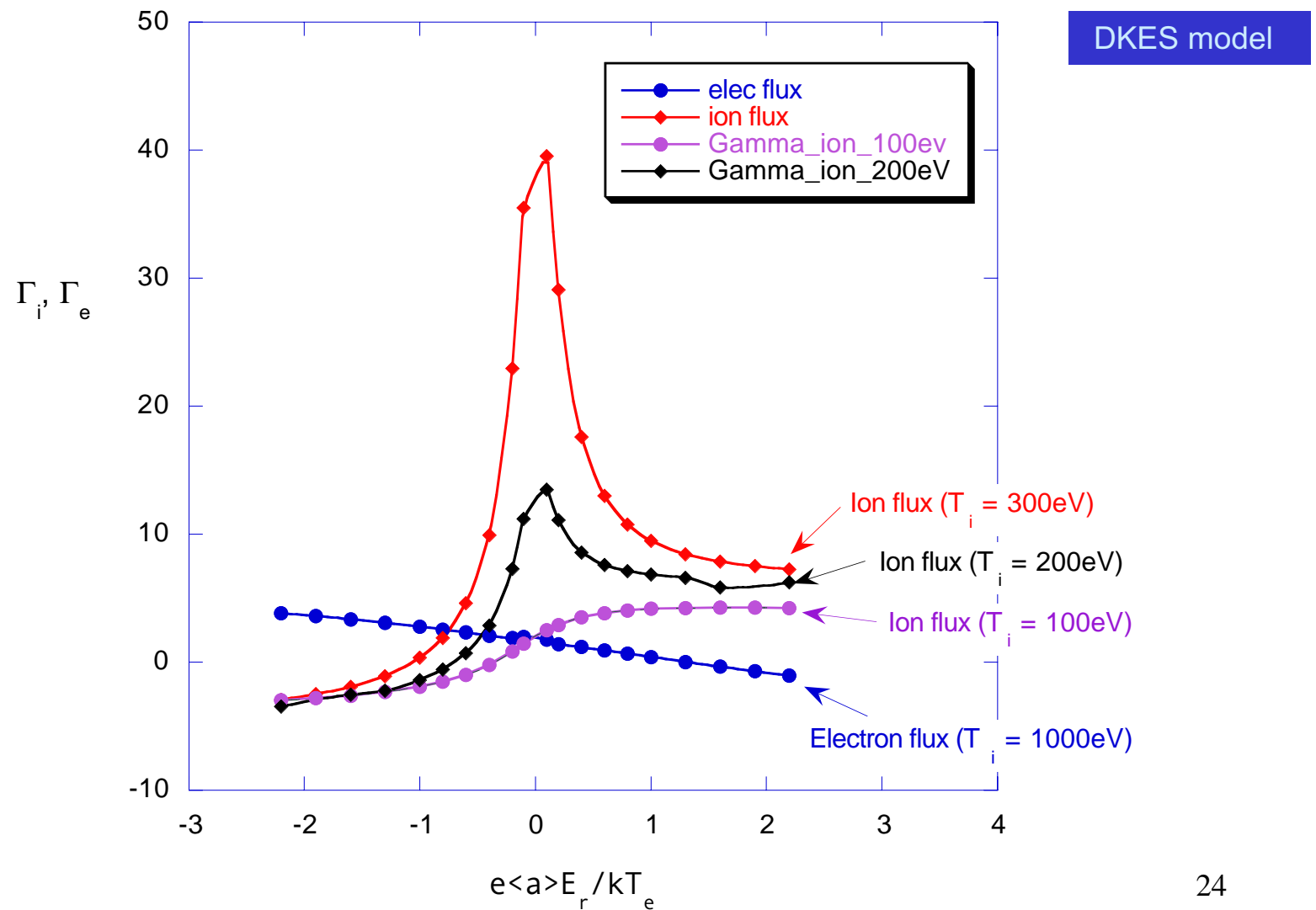
$$L_{ij} = L_{ij} \left(\frac{v}{v}, \frac{E_r}{v} \right)$$

(i.e., to carry out the above integrals, one will need to generate a 2-D matrix of Γ 's vs. these parameters for each flux surface)

This model is motivated by the more complete DKES calculations that indicate electrons are generally in the $1/v$ regime:

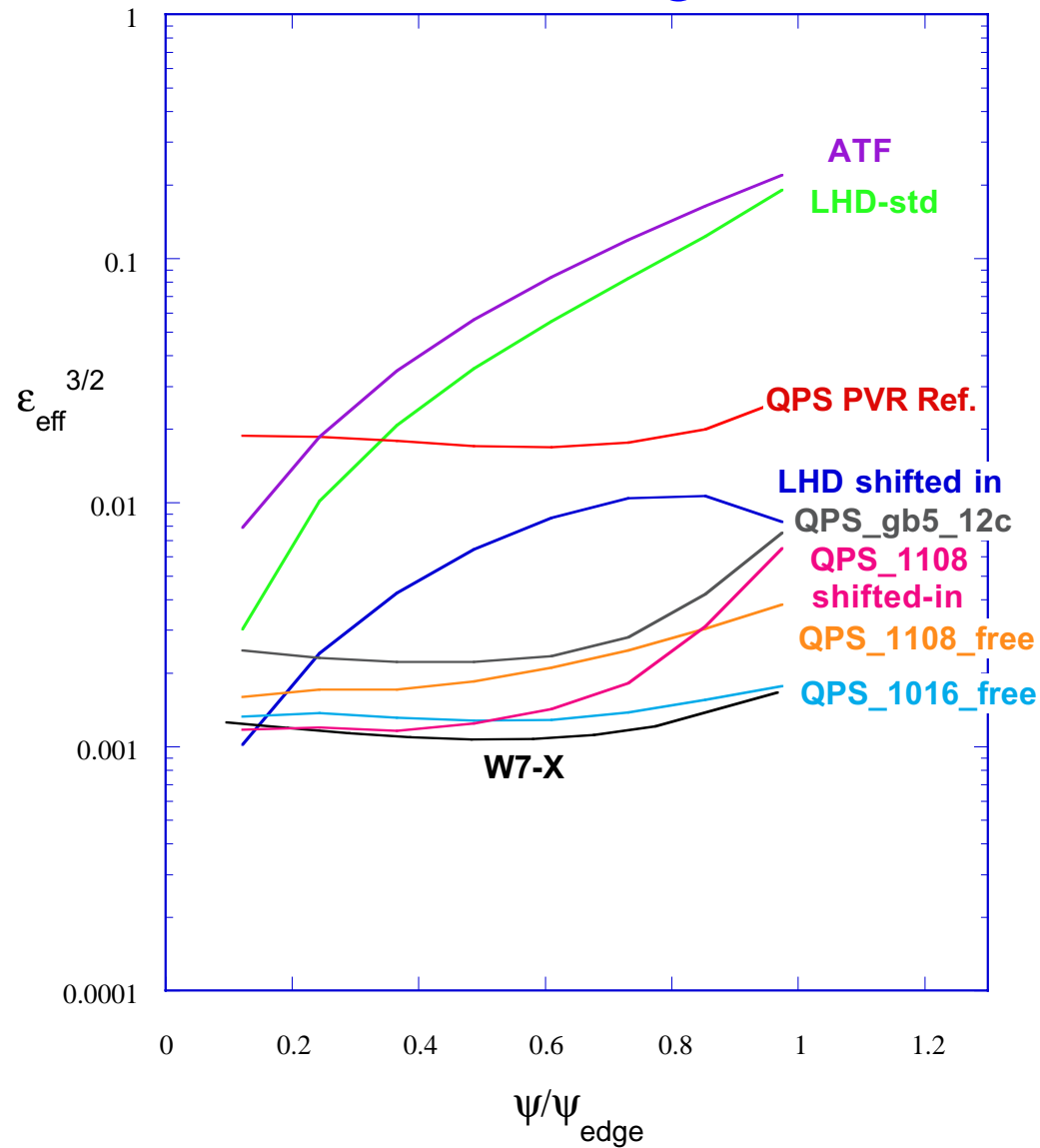


Typical DKES ambipolar calculations also show that overall transport level is generally set by lowering ion flux down to that of the electrons.

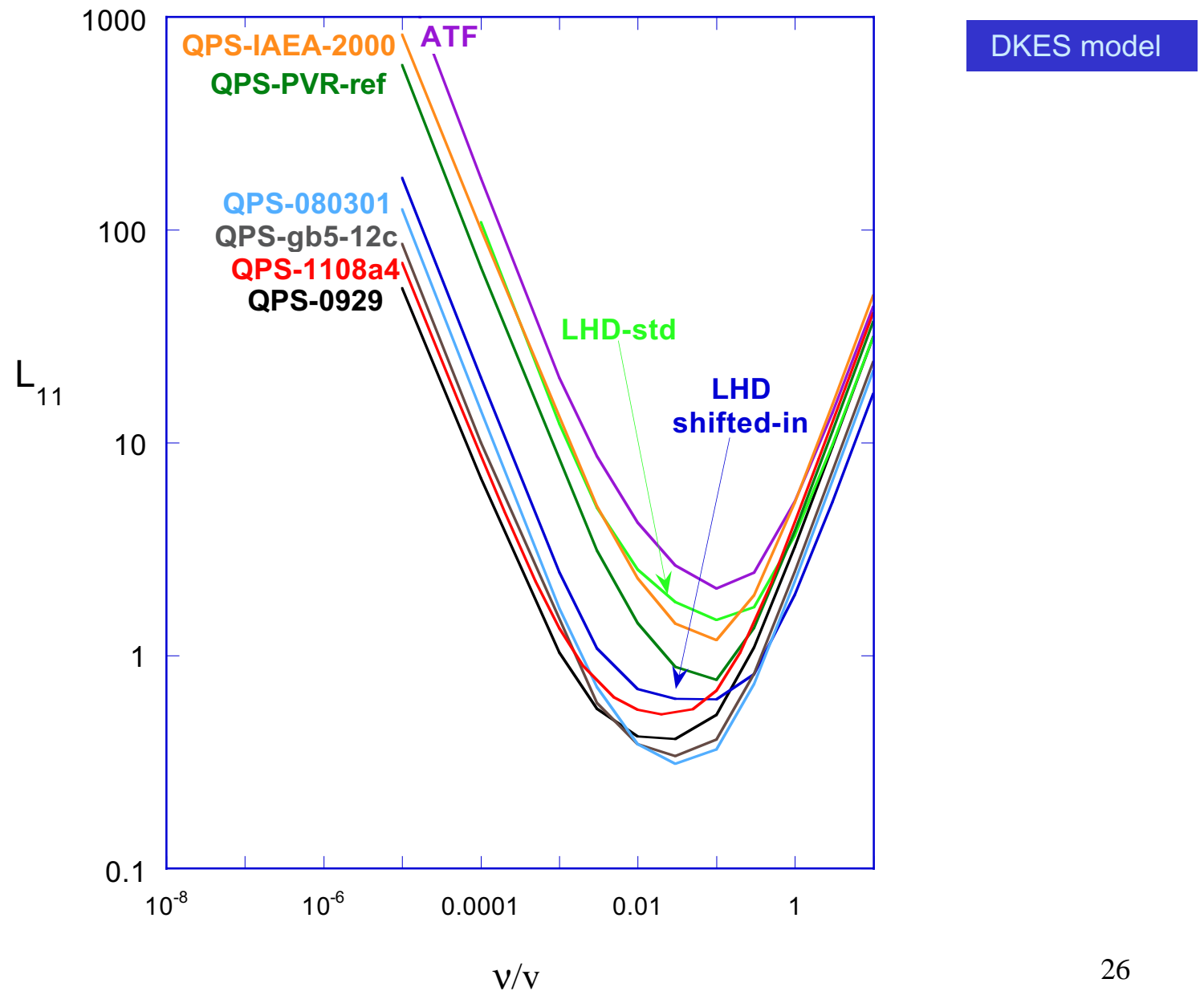


NEO code provides $\epsilon_{\text{eff}}^{3/2} \sim D^{1/\nu}, \chi^{1/\nu}$. Demonstrates effectiveness of NEO/DKES optimizations over a series of configurations

NEO ϵ_{eff} code

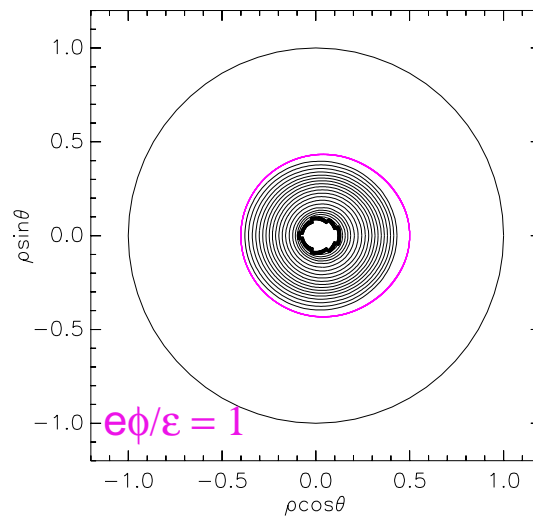
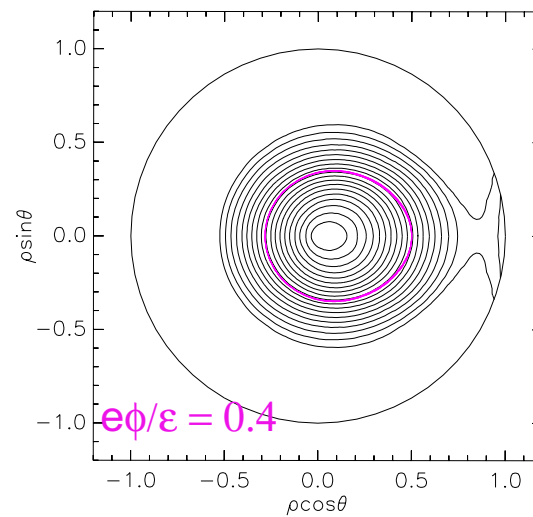
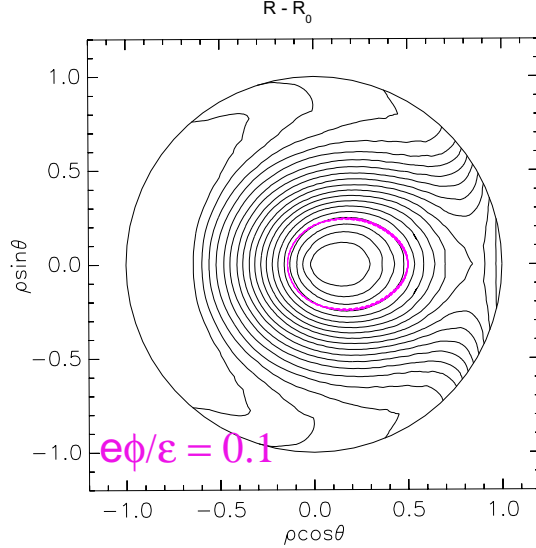
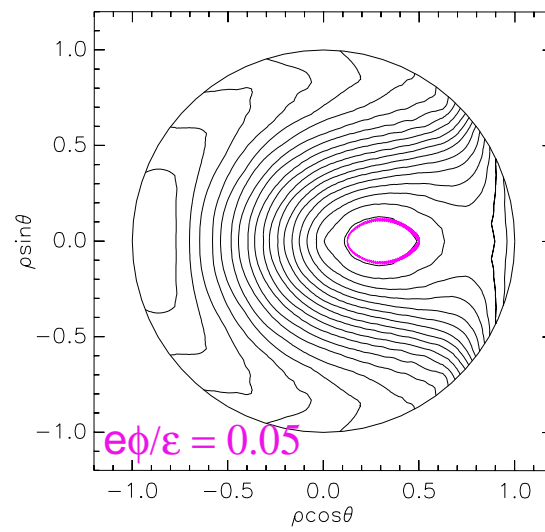
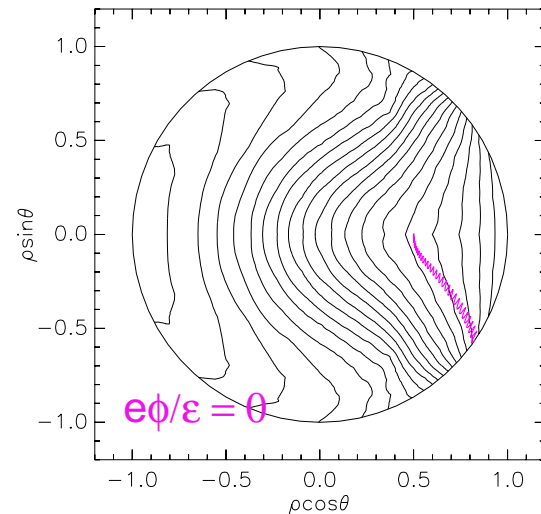
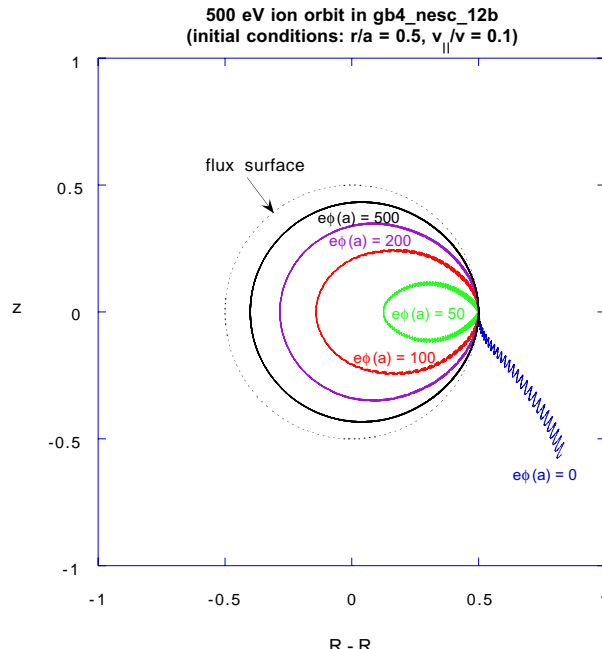


DKES L_{11} transport coefficient at $E_r/v = 0.0001$ show similar trends at low collisionality among gb4/gb5 devices as NEO $\epsilon_{\text{eff}}^{3/2}$ coefficient

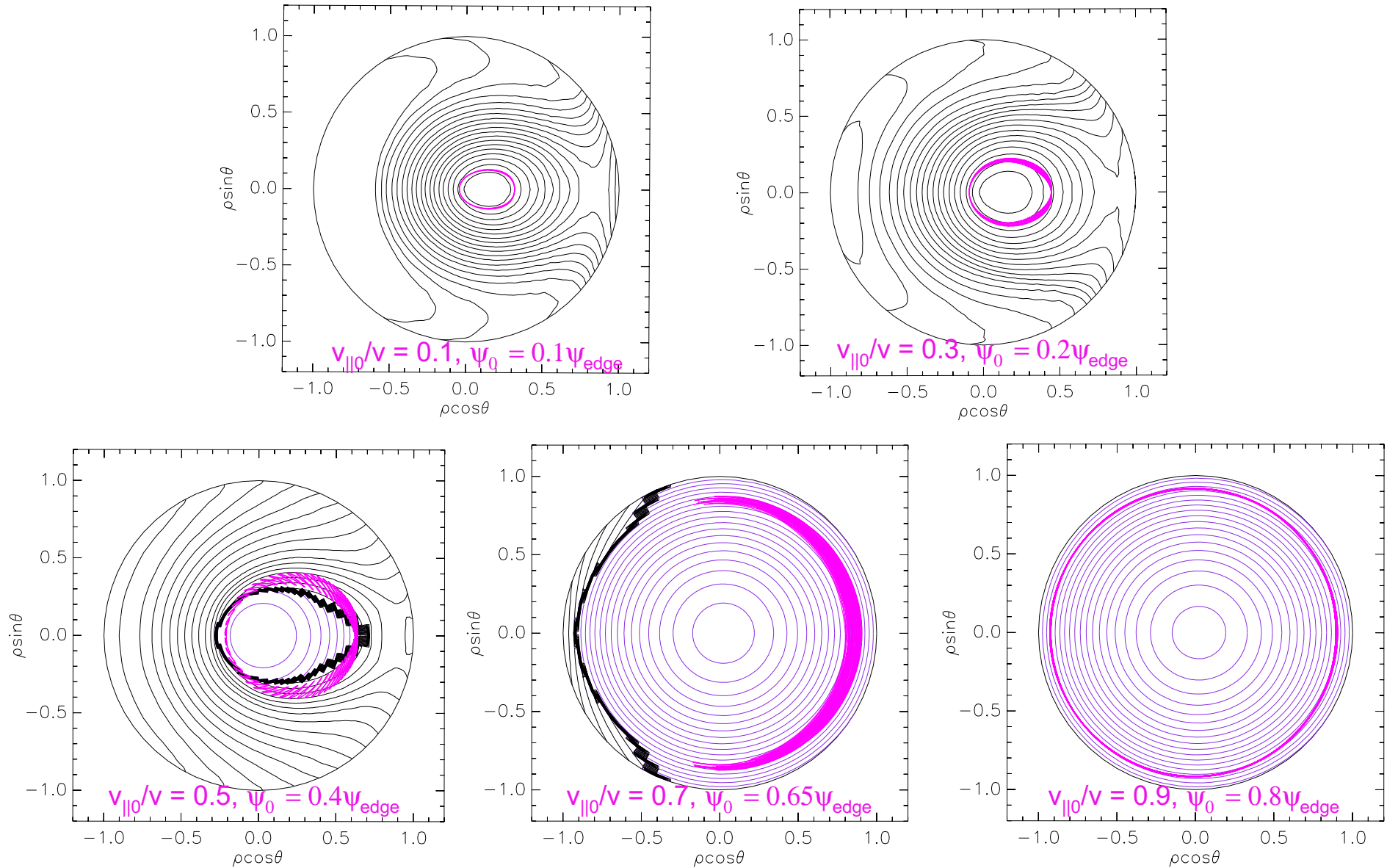


QPS ORBITS AND MONTE CARLO SIMULATION

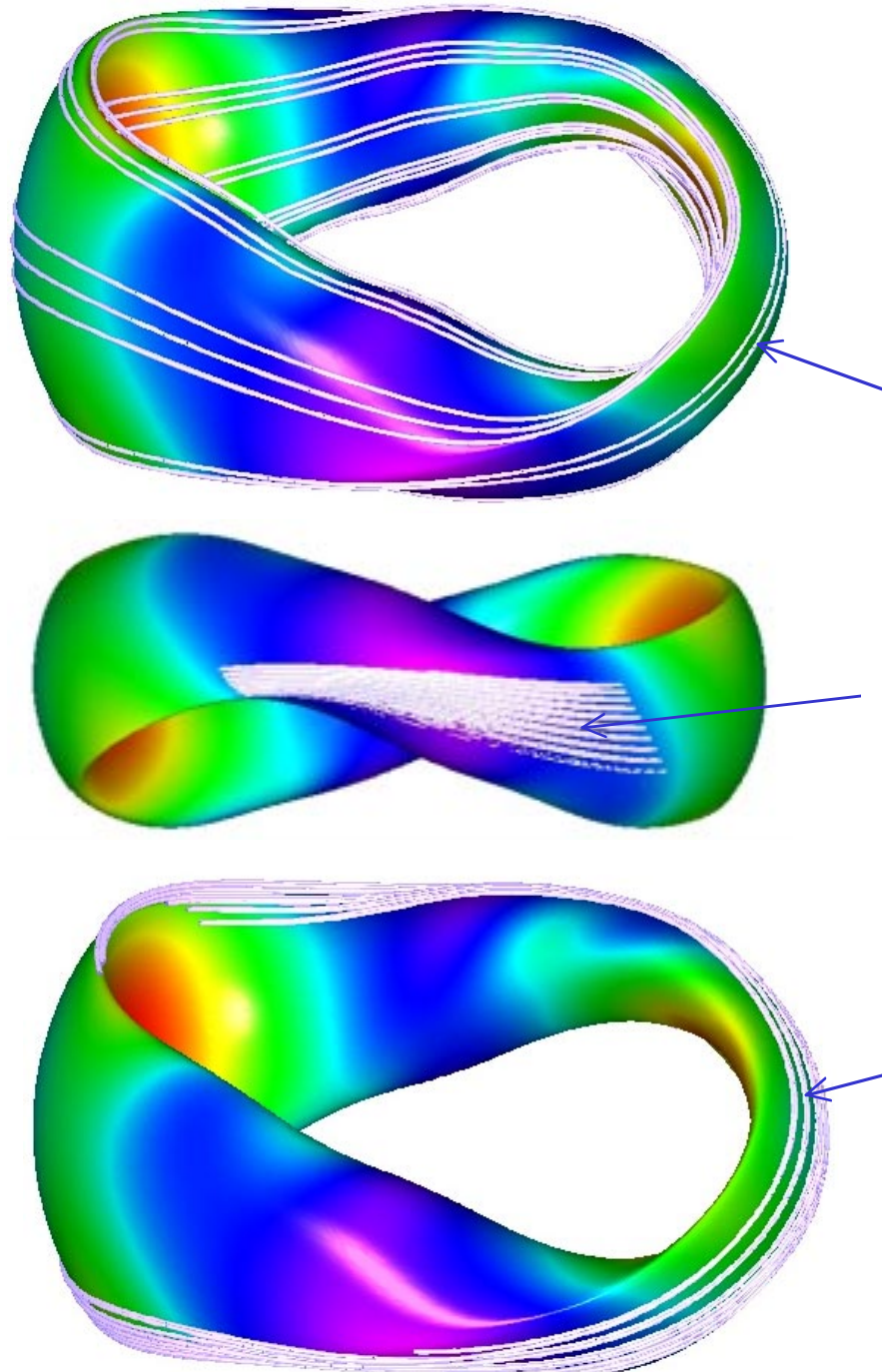
Improvement of trapped 500 eV ion orbits with electric fields and alignment with J^* contours



Alignment of $v_{||0}/v = 0.1, 0.3, 0.5, 0.7, 0.9$ 500 eV ion orbits with J^* contours
 (black contours = locally trapped, purple contours = passing, magenta = orbit)



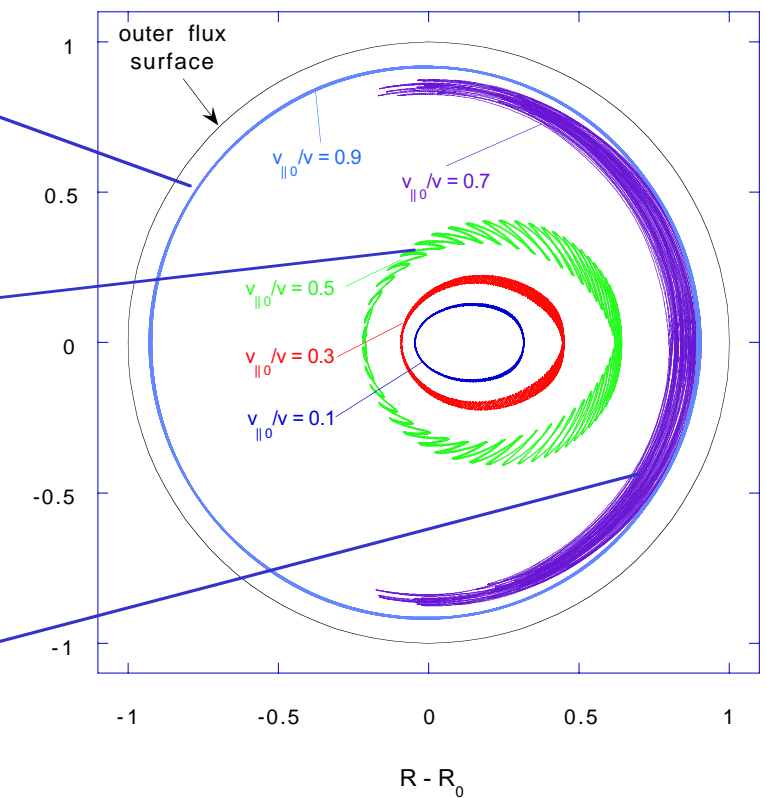
QPS orbit topologies



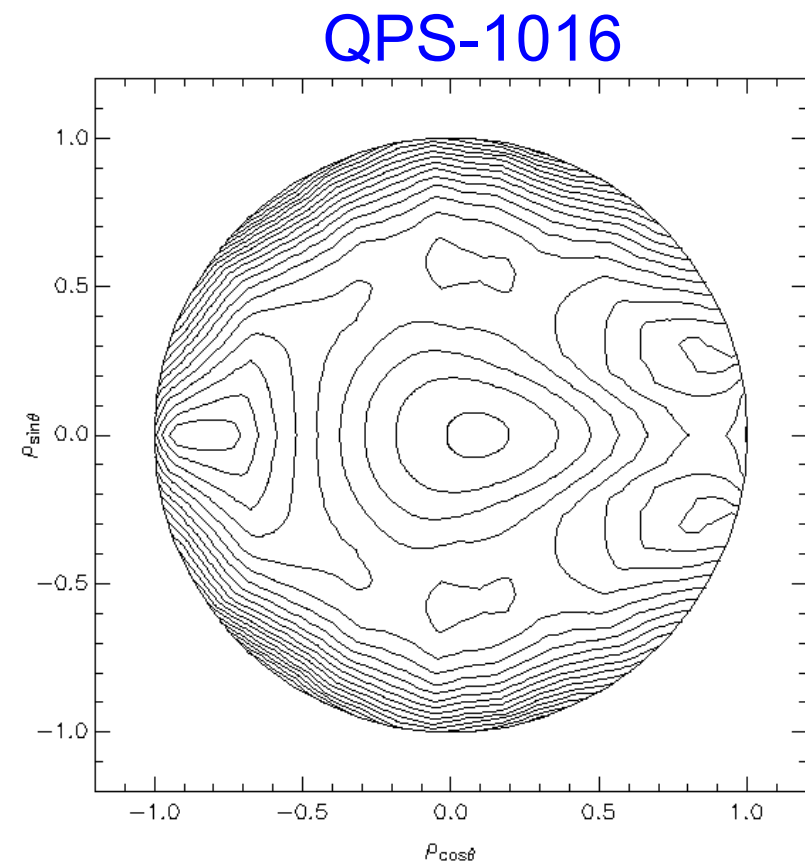
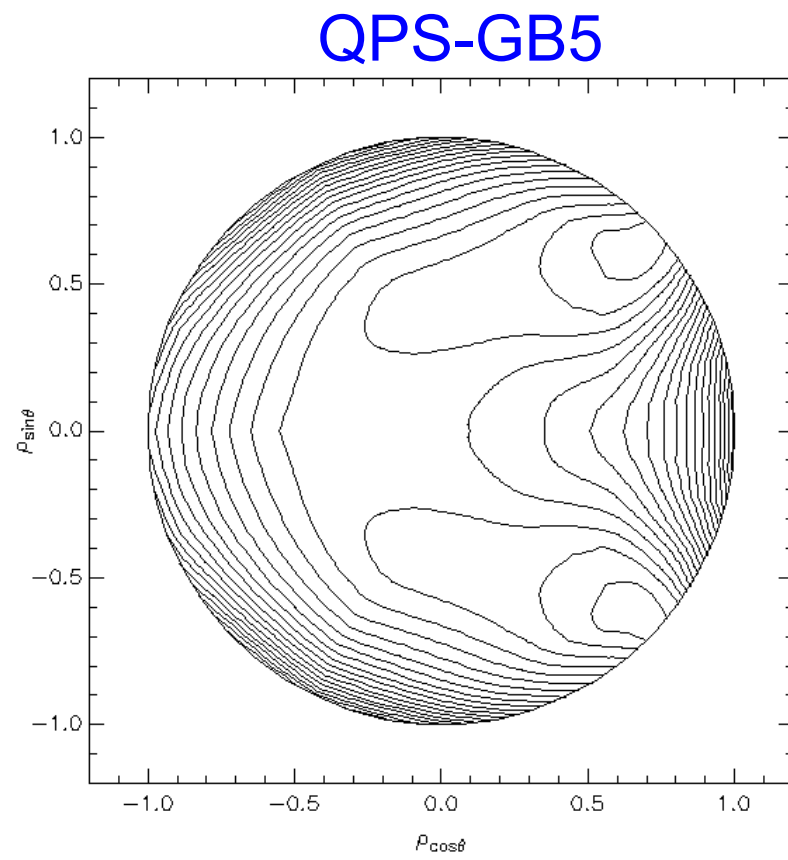
Passing

Helically trapped

Toroidally trapped

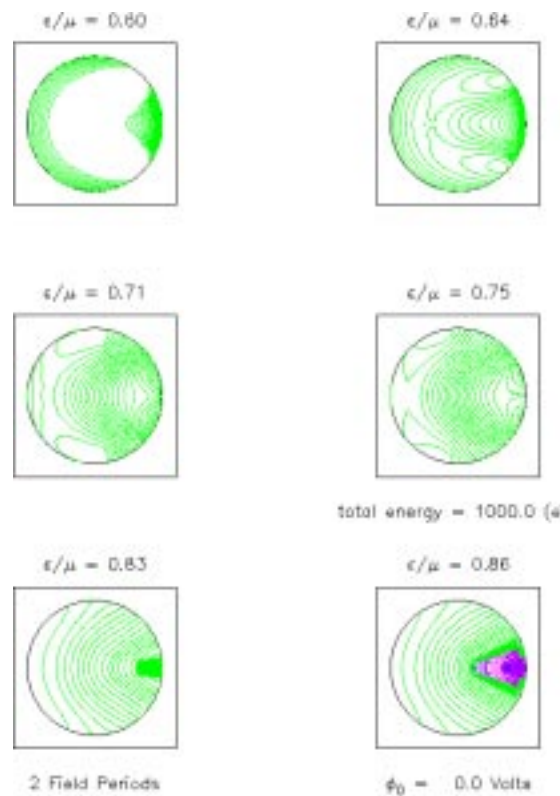


The recent QPS-1016 configuration improves the closure and centering of B_{\min} contours:

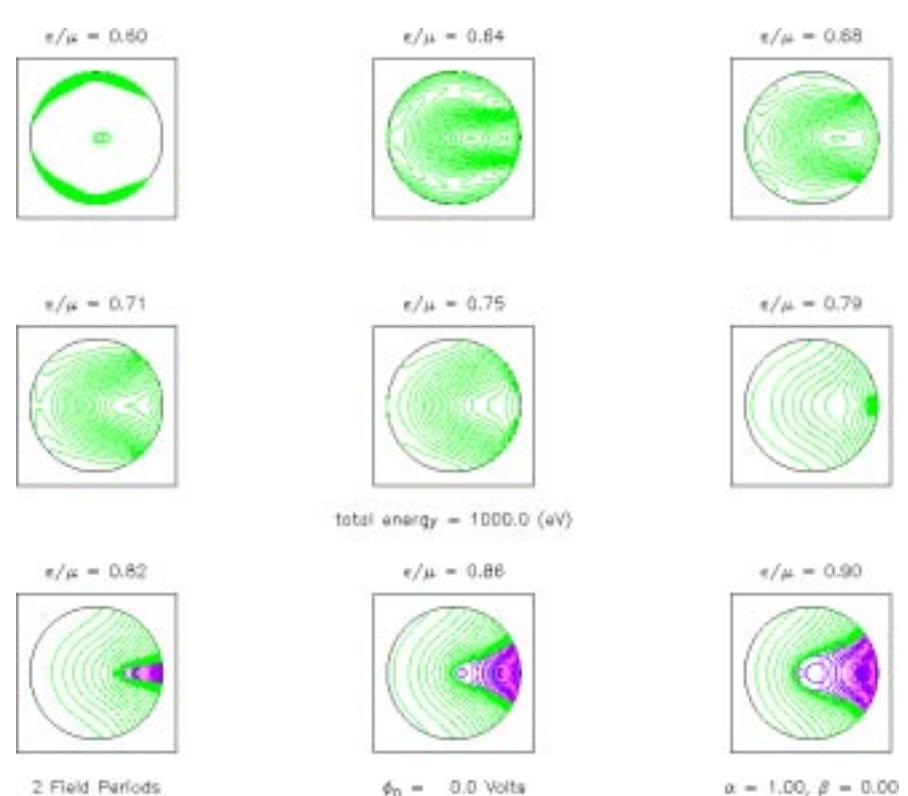


QPS-1016 also improves closure of the deeply trapped J^* contours ($\epsilon/\mu < 0.7$)

QPS-GB5



QPS-1016

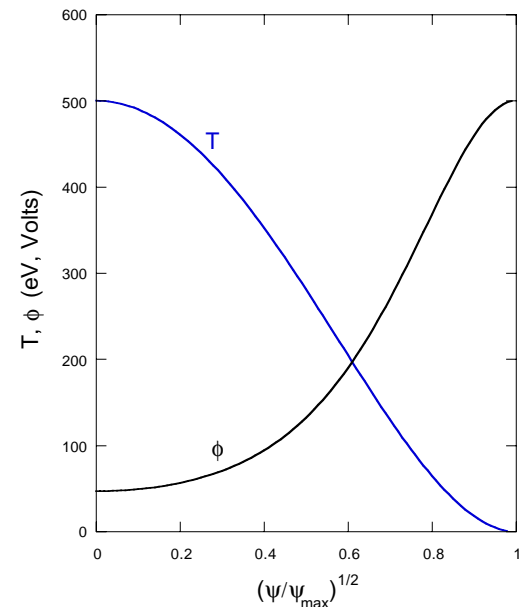
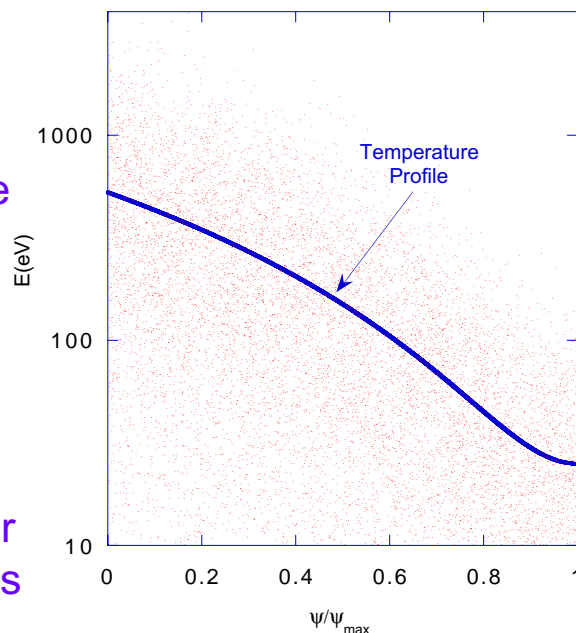


Monte Carlo procedure for estimating global energy lifetimes (DELTA5D code)

DELTA5D Monte Carlo

- start with particles distributed over cross section using PDF's consistent with assumed profiles and local Maxwellians
- follow ensemble in time, replacing particles (consistent with initial PDF's) as they leave outer surface
- Record energies of escaping particles - use to calculate τ_E
- Follow until approximate steady-state is achieved
- Vary potential (with fixed profile shape) to achieve global ambipolar balance of electron/ion particle loss rates

Typical initial Maxwellian particle loading for $T = 500\text{eV}$ $(1 - \psi/\psi_{\max})^2$



Power flows for global single species test particle simulations:

- To achieve steady state, in a reasonable simulation time, terms (1) and (2) need to be balanced:
- For $E_r = 0$

- can include pitch angle and energy scattering if $Q_{ii} + Q_{ei}$ is weak during particle confinement time
- or can include only pitch angle scattering

- For $E_r \neq 0$
 - rely on $Q_{ii} + Q_{ei}$ term (1) to redistribute energy loss/gain from term (2)
 - or can remove kinetic energy loss/gain (due to $e\Delta\phi$) each time step

DELTA5D Monte Carlo

$$\frac{dW_{test,ion}}{dt} = \int (Q_{ii} + Q_{ei}) d^3v \quad (+/-) \quad (1)$$

$$+ \int \vec{J} \bullet \vec{E} d^3v \quad (+/-) \quad (2)$$

$$+ \int \frac{dW_{surface-loss}}{dt} dS \quad (-) \quad (3)$$

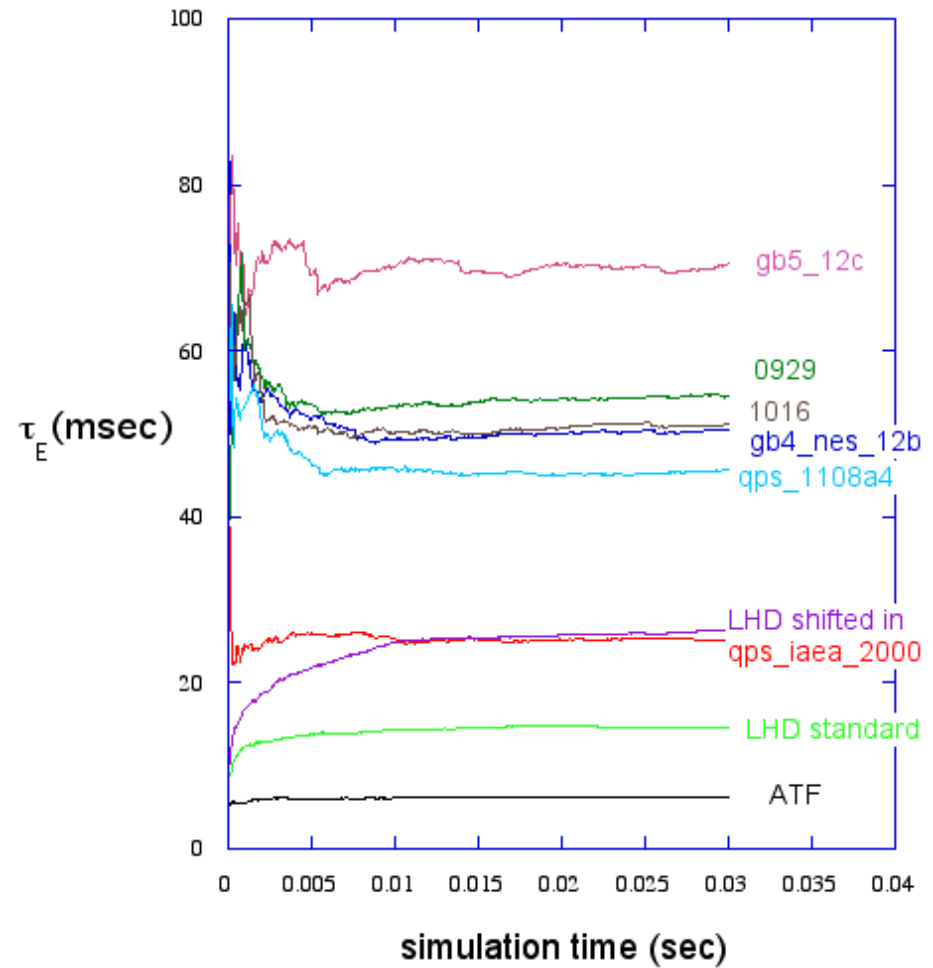
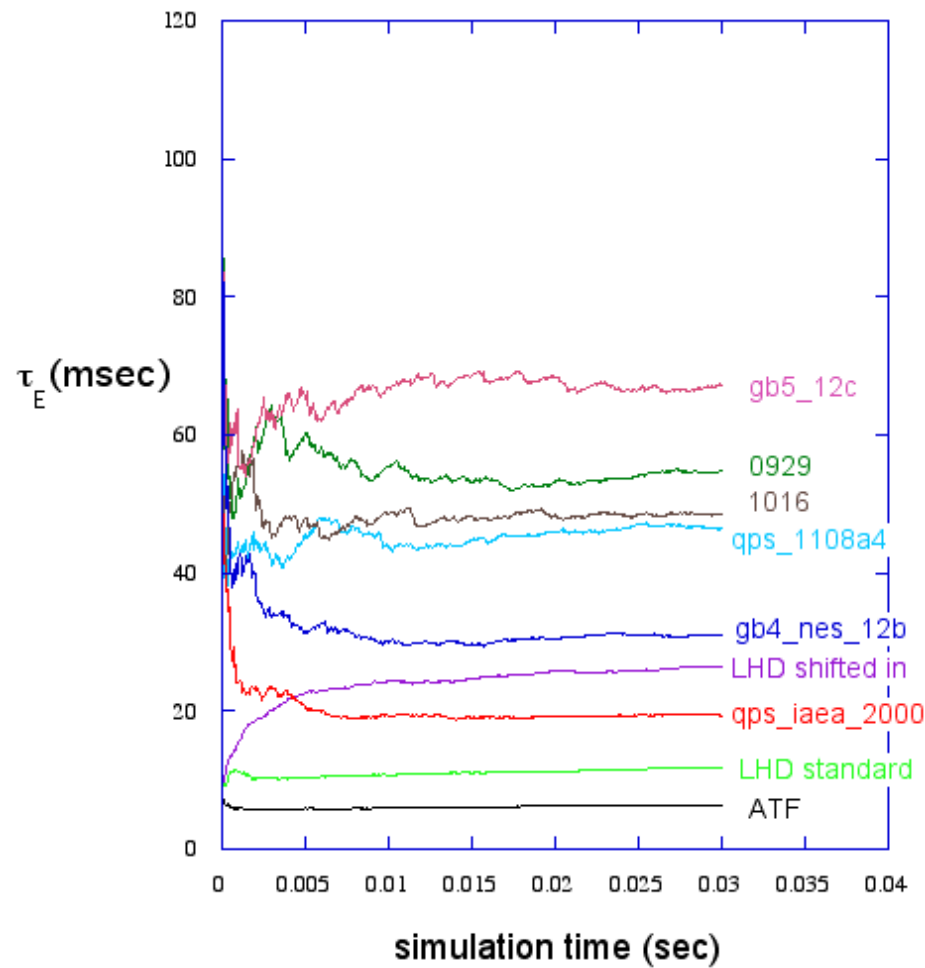
$$+ \int N_{replacement} [T(\psi) + e\phi] d^3v \quad (+/-) \quad (4)$$

$$\frac{dW_{test,electron}}{dt} = \text{Similar equations}$$

Comparison of Ion Monte Carlo lifetimes among different configurations (all scaled to constant R_{\max} and $\langle B \rangle$)

ECH regime: $n(0) = 1.8 \times 10^{19} \text{ m}^{-3}$, $T_e(0) = 1400 \text{ eV}$, $T_i(0) = 150 \text{ eV}$

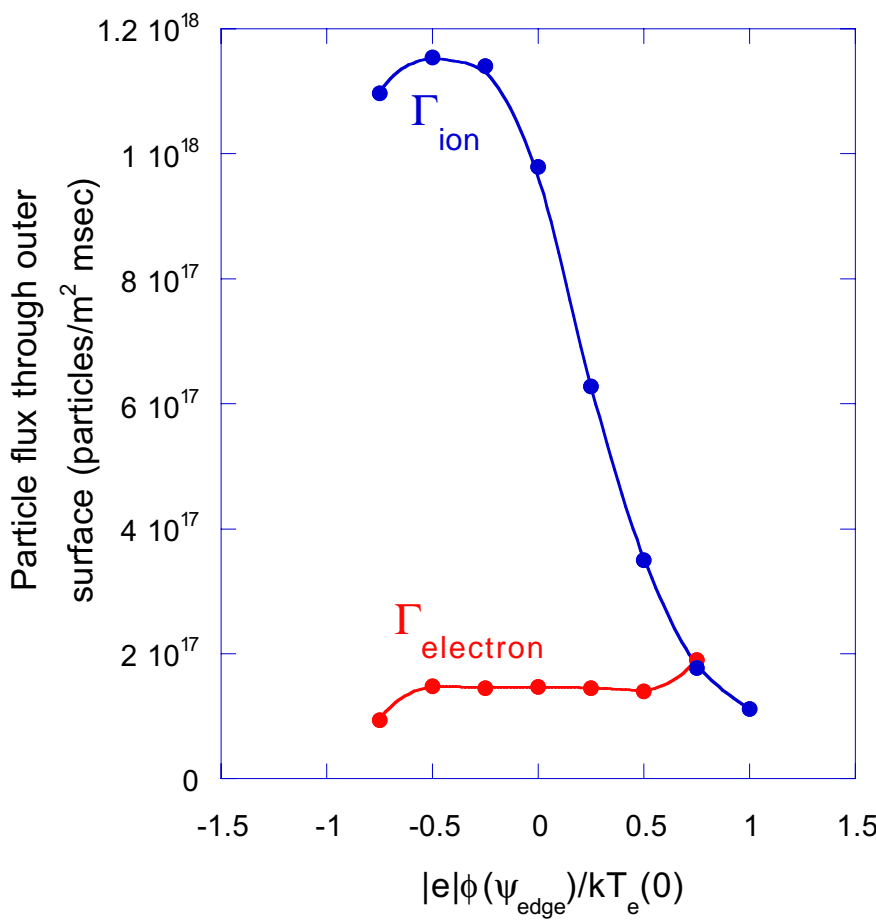
ICH regime: $n(0) = 8.3 \times 10^{19} \text{ m}^{-3}$, $T_e(0) = 500 \text{ eV}$, $T_i(0) = 500 \text{ eV}$



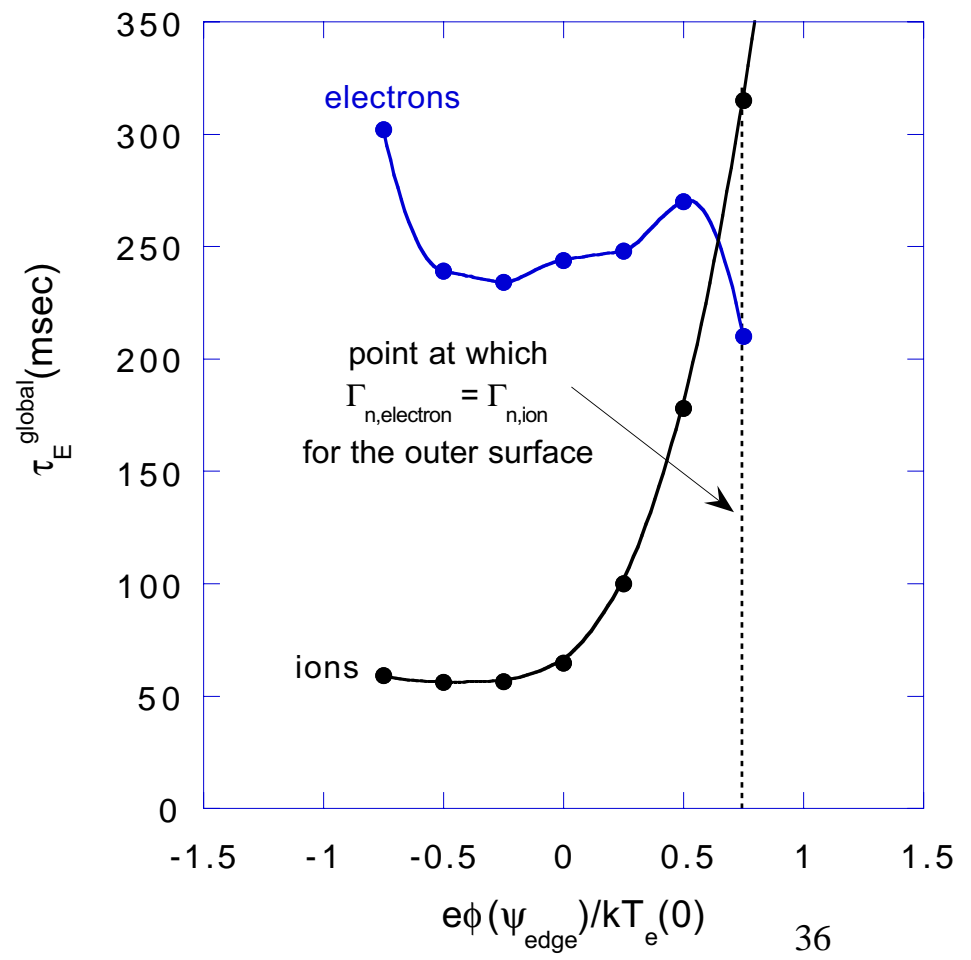
Monte Carlo lifetimes for ICH heated gb4 configuration

$[n(0) = 8.3 \times 10^{19} \text{ m}^{-3}, T_e(0) = 500 \text{ eV}, T_i(0) = 500 \text{ eV, flat density profile, parabolic}^{**2} \text{ temperature profile}]$

Global ambipolarity condition [i.e., with $\phi(r)$ profile fixed]



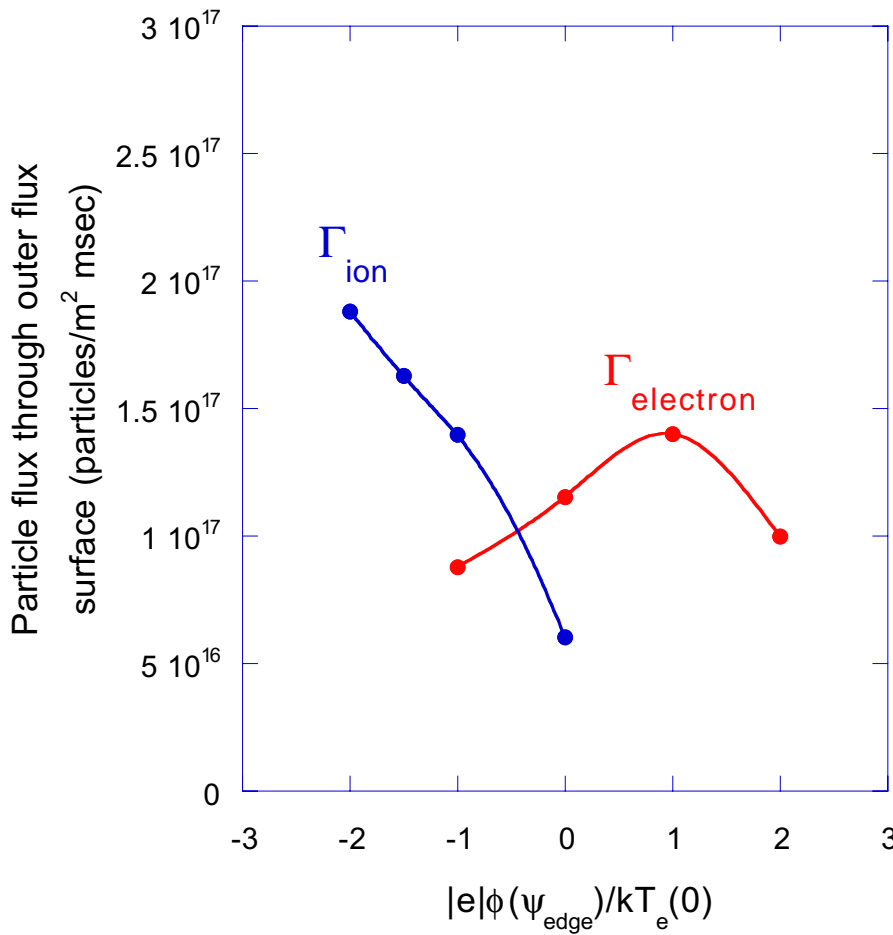
Global electron/ion energy lifetimes



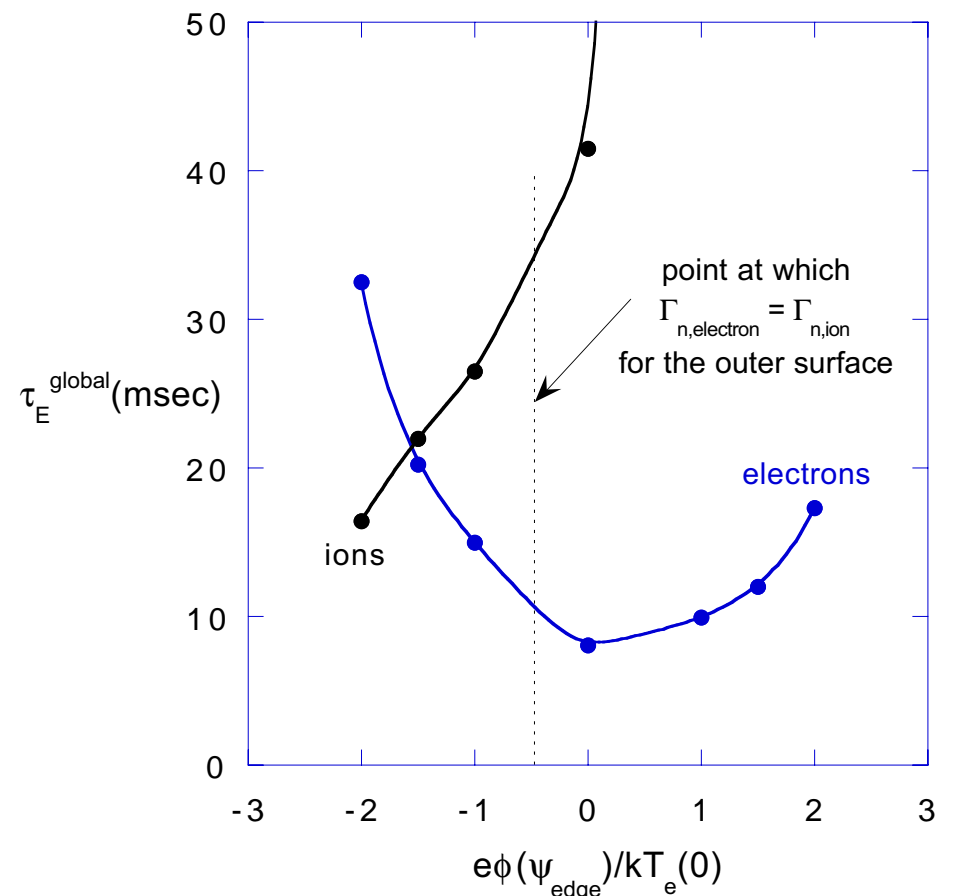
Monte Carlo lifetimes for ECH heated gb4 configuration

[$n(0) = 1.8 \times 10^{19} \text{ m}^{-3}$, $T_e(0) = 1400 \text{ eV}$, $T_i(0) = 150 \text{ eV}$, flat density profile, parabolic**2 temperature profile]

Global ambipolarity condition
[i.e., with $\phi(r)$ profile fixed]



Global electron/ion energy lifetimes

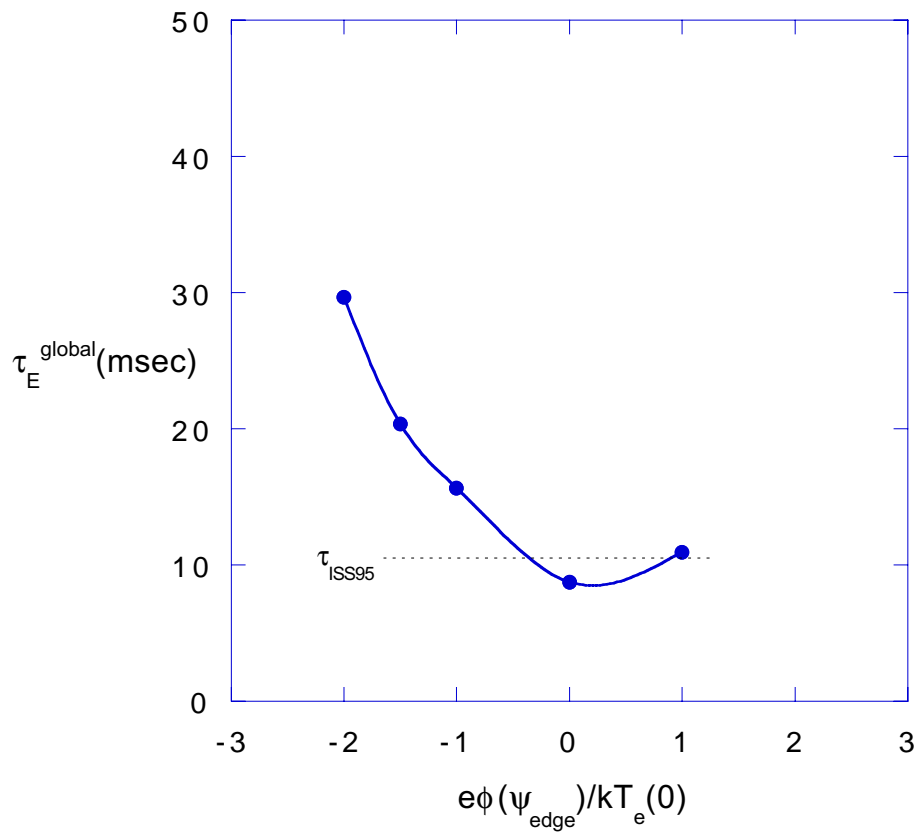


Comparison of ECH/ICH global lifetimes with ISS95 scaling law for GB4 configuration

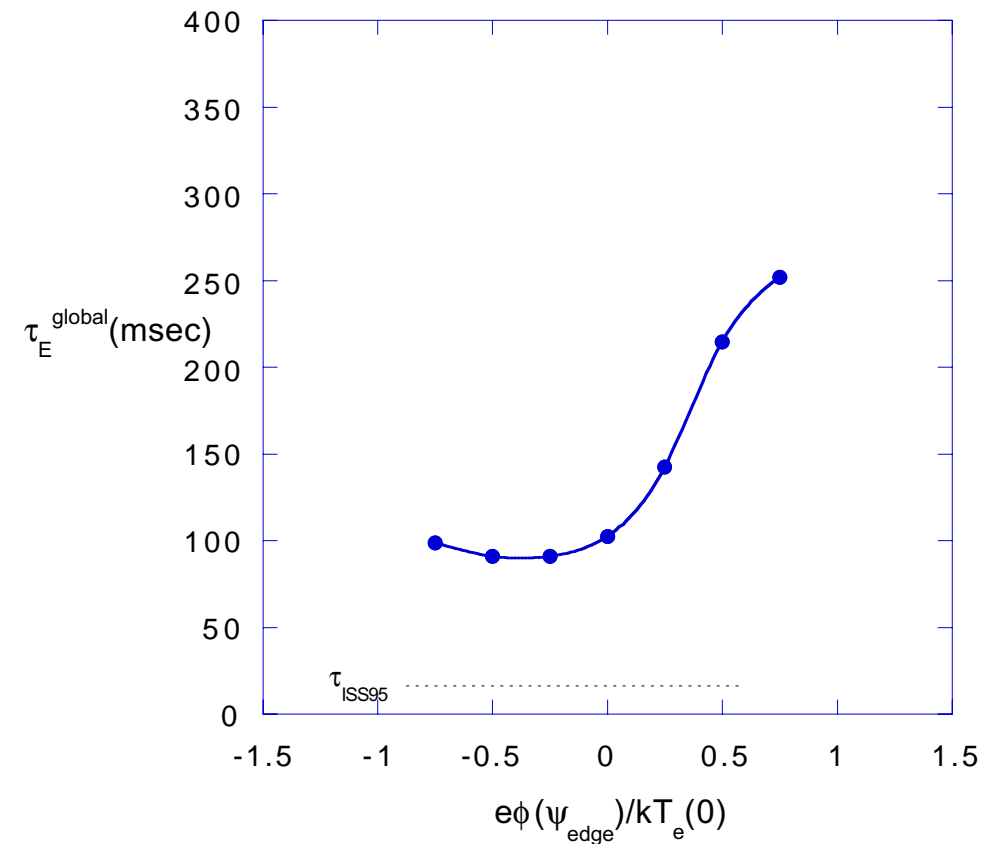
τ_{gl}^{MC} = global lifetime, taking into account electron and ion loss channels:

$$\tau_{gl}^{MC} = \frac{(T_e + T_i)\tau_e\tau_i}{T_e\tau_i + T_i\tau_e}$$

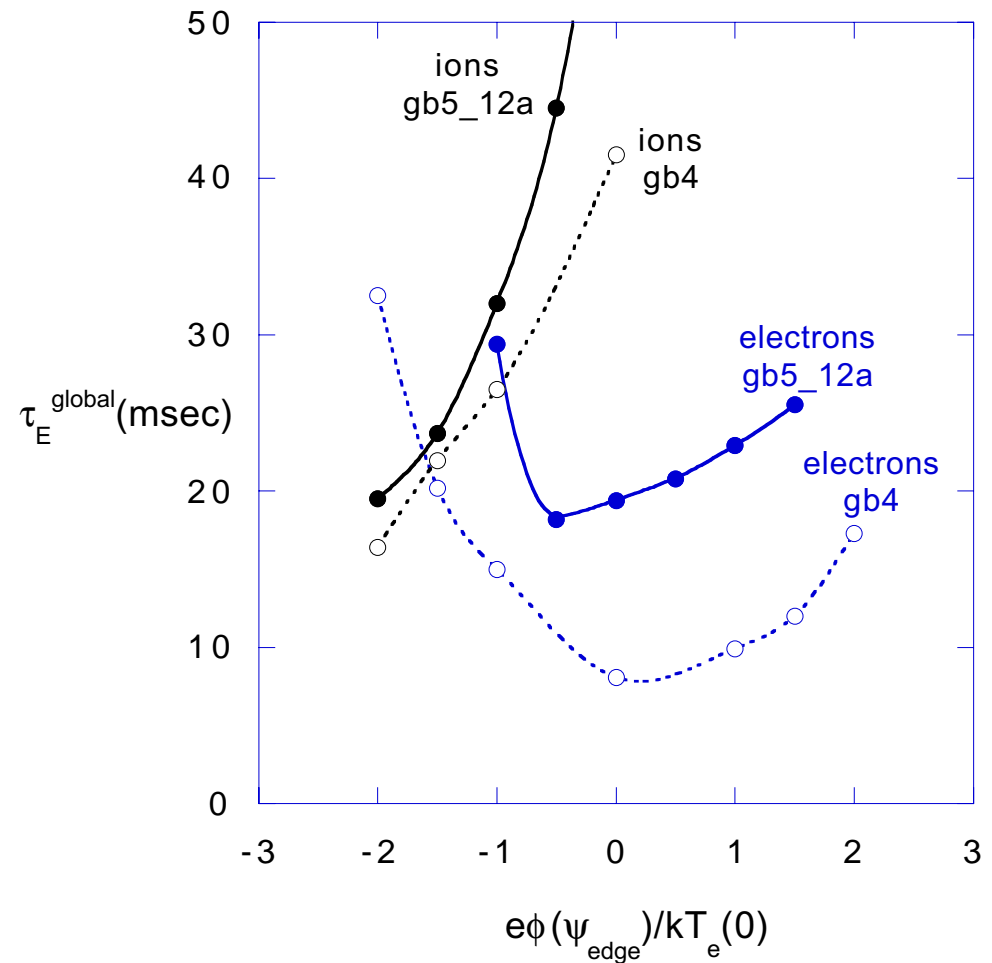
ECH heated gb4 case



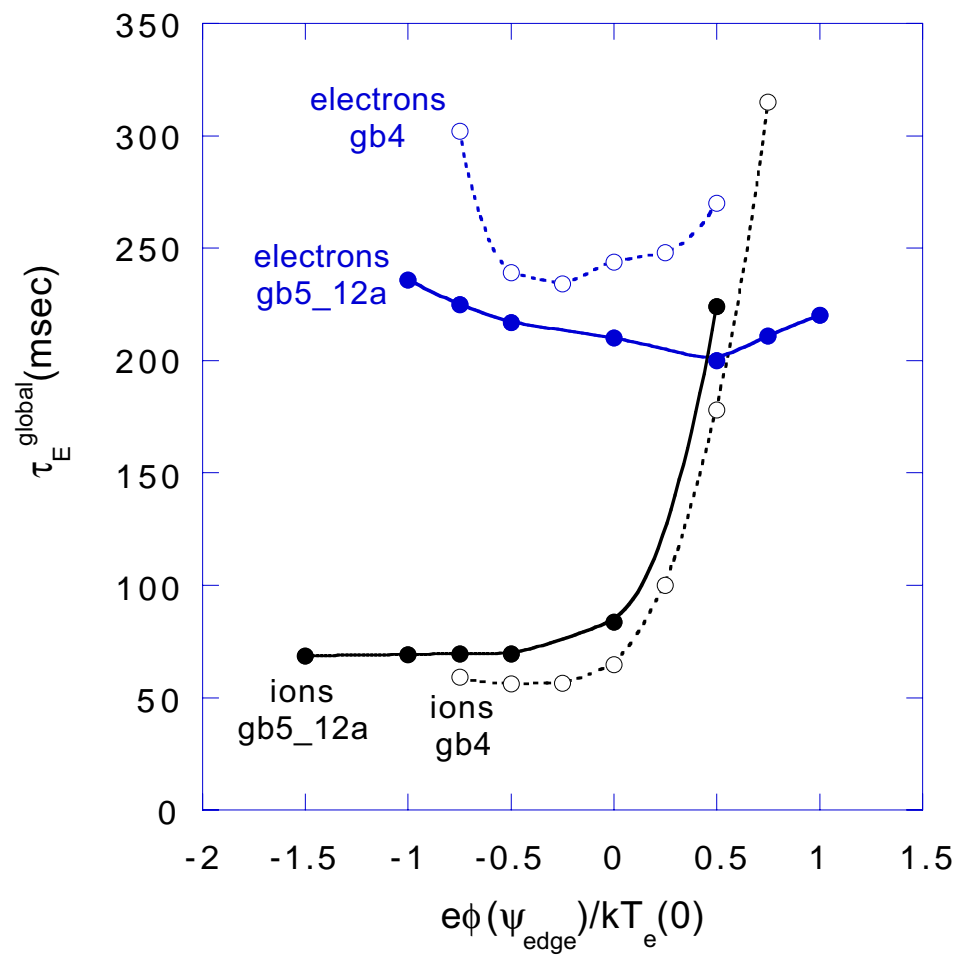
ICH heated gb4 case



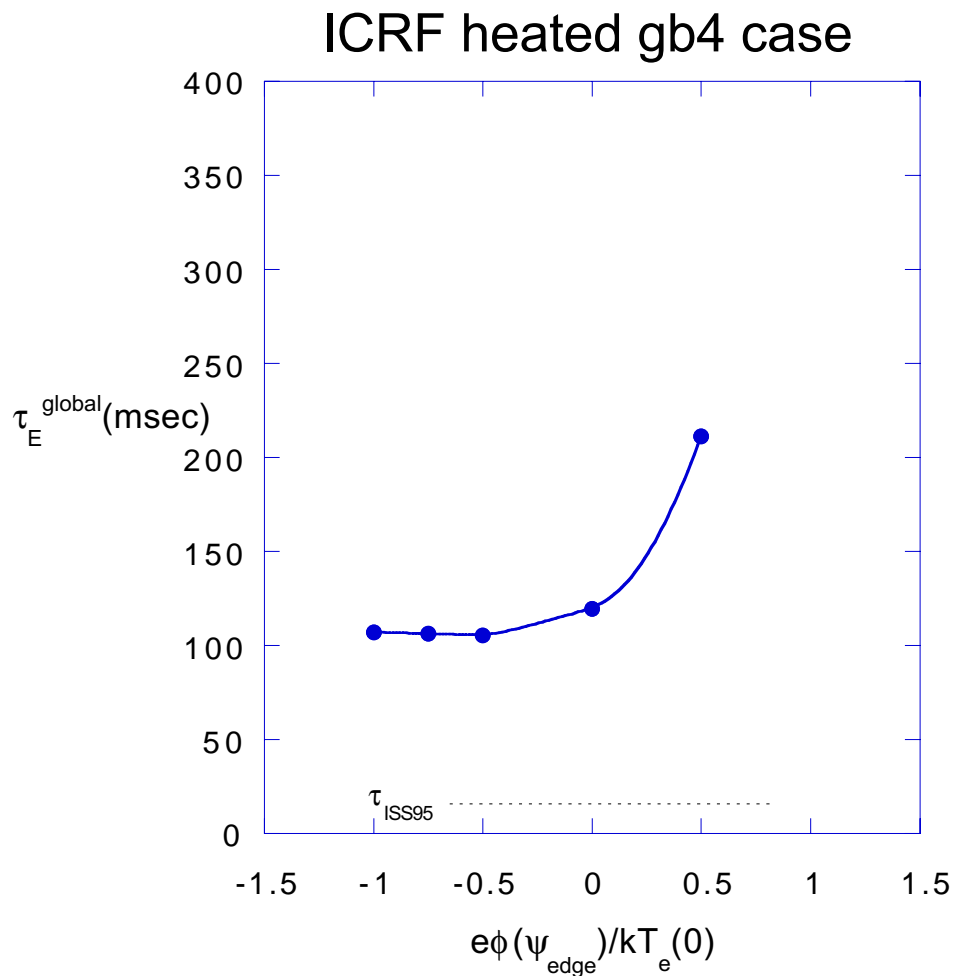
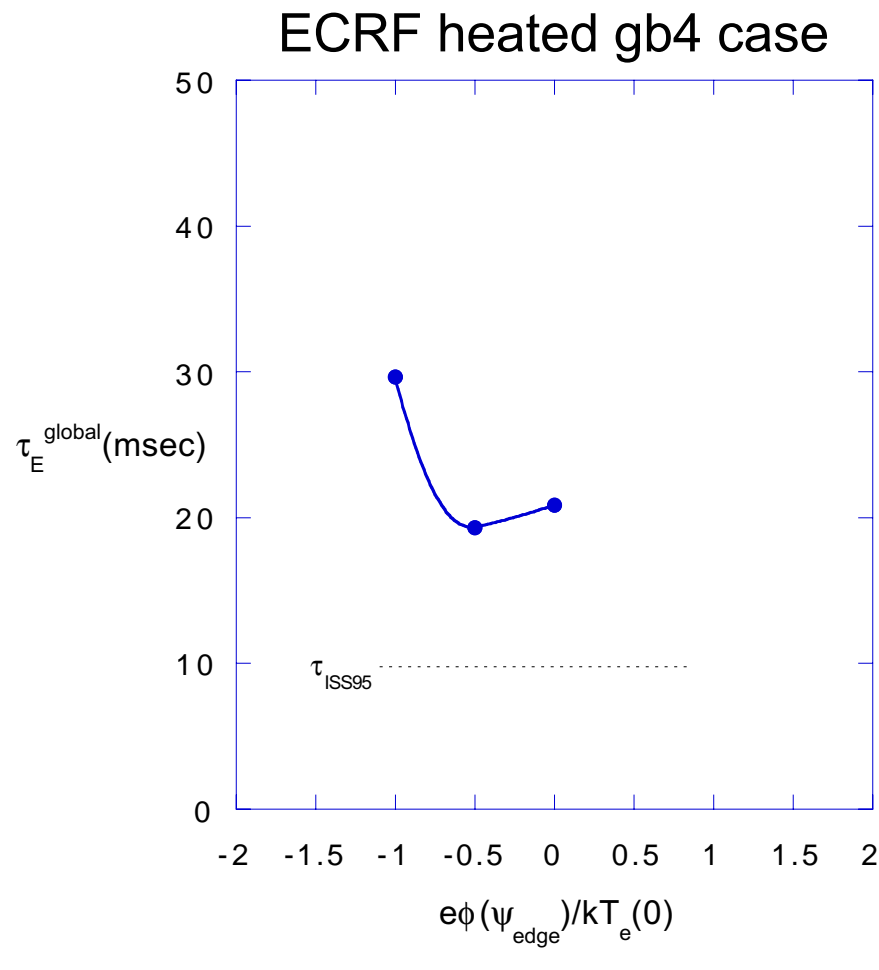
Comparison of gb4 and gb5 global lifetimes for ECH parameters



Comparison of gb4 and gb5 global lifetimes for ICH parameters

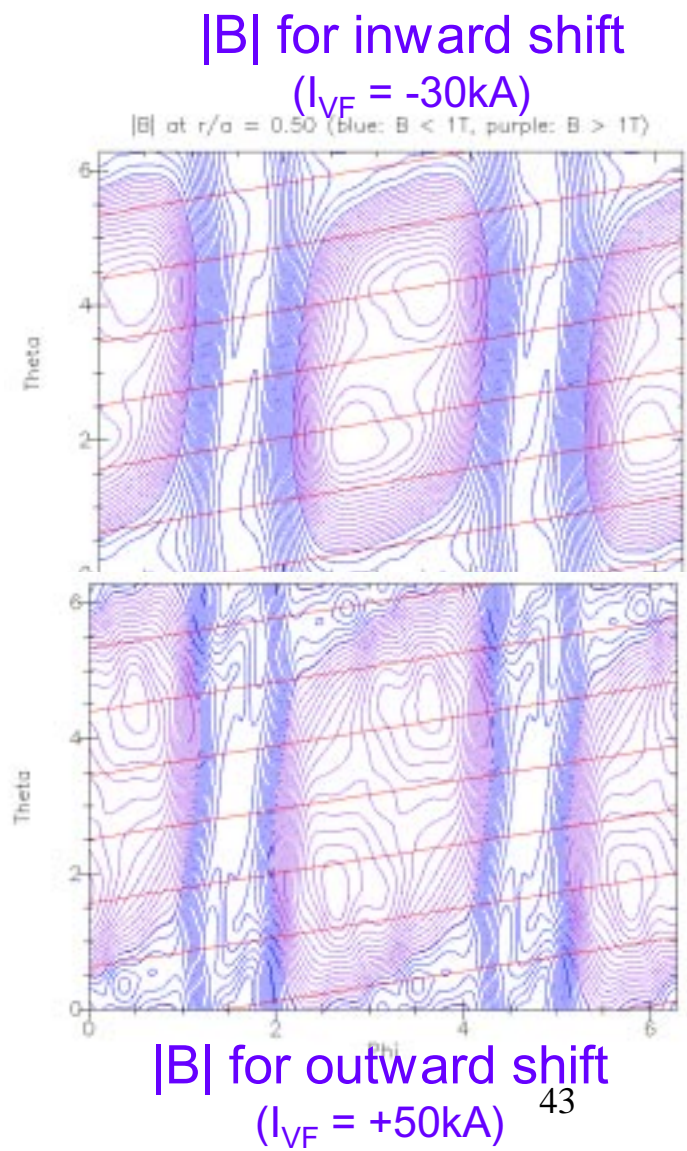
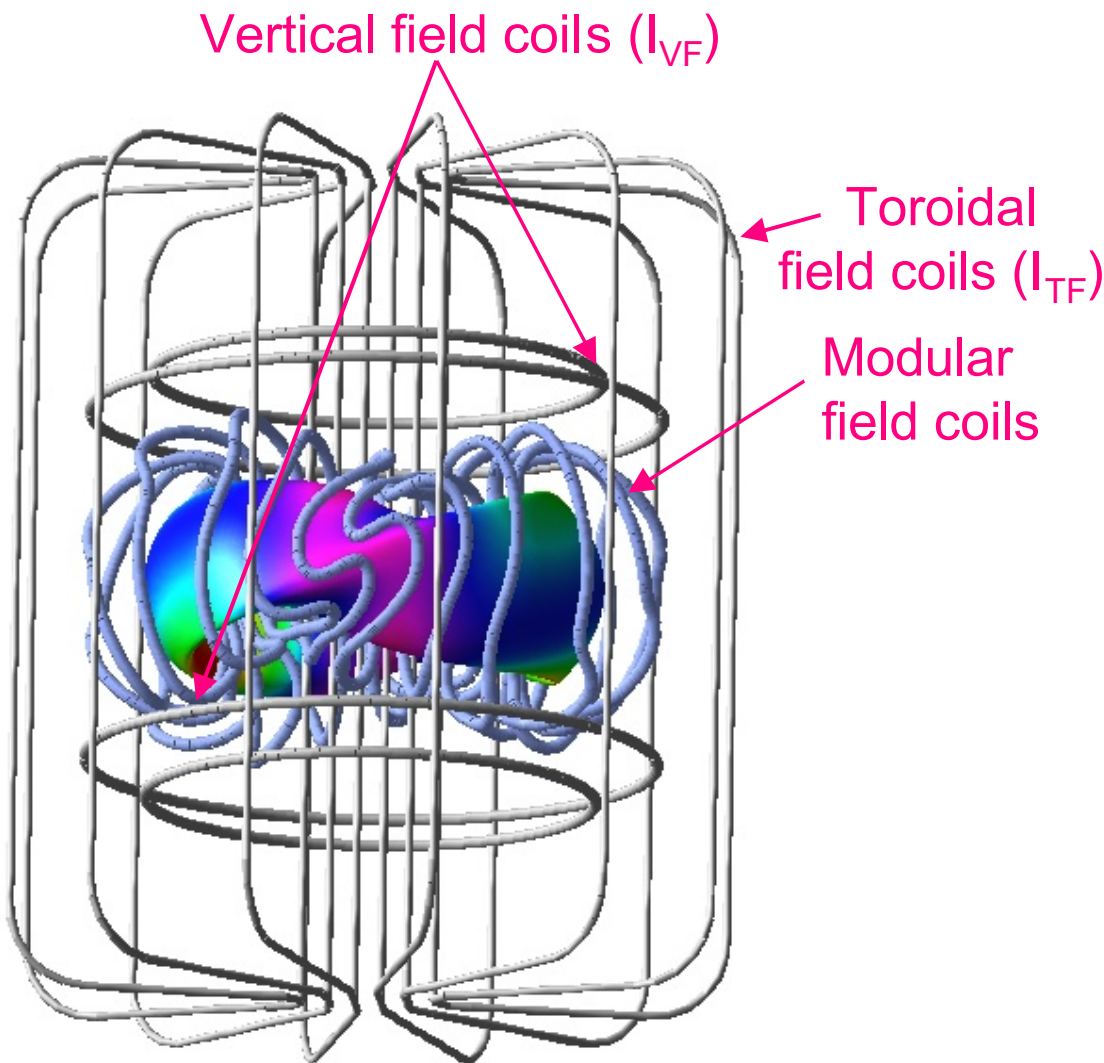


Comparison of ECH/ICH global lifetimes with ISS95 scaling law for GB5_12A configuration

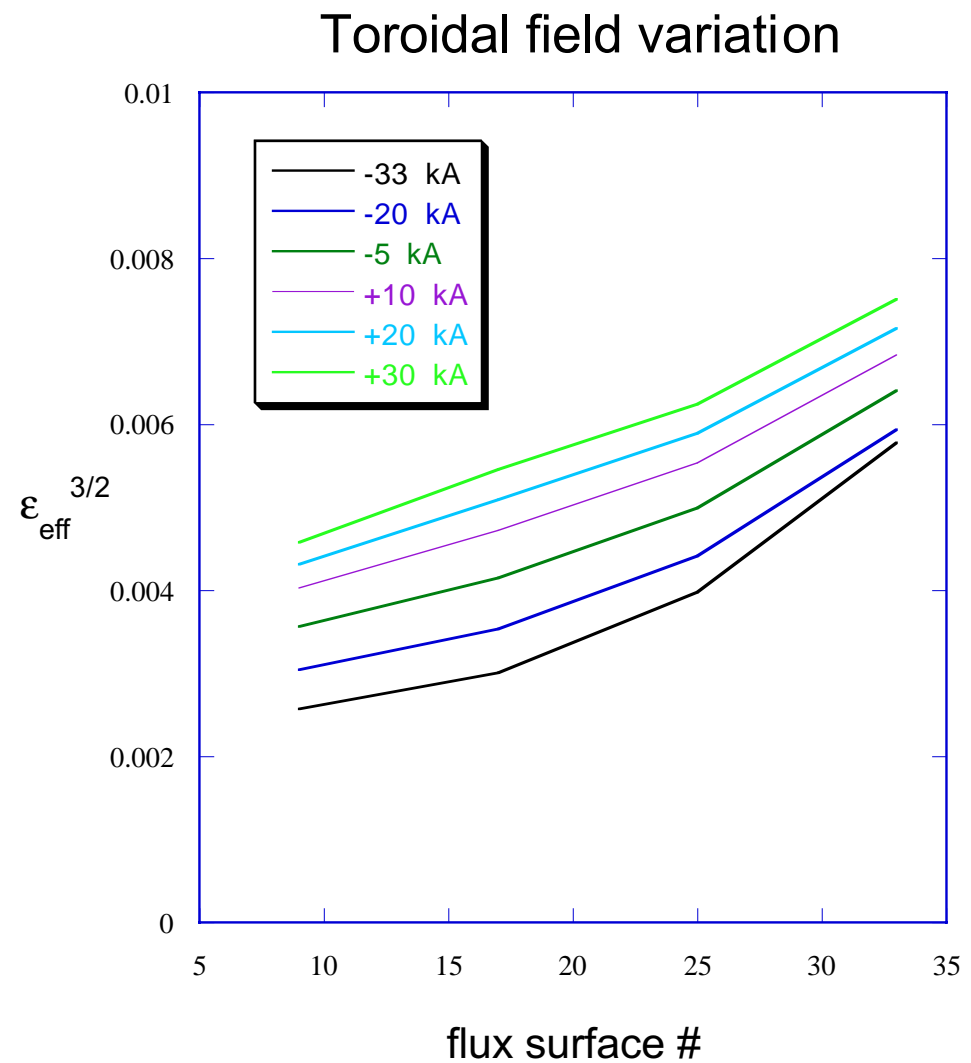
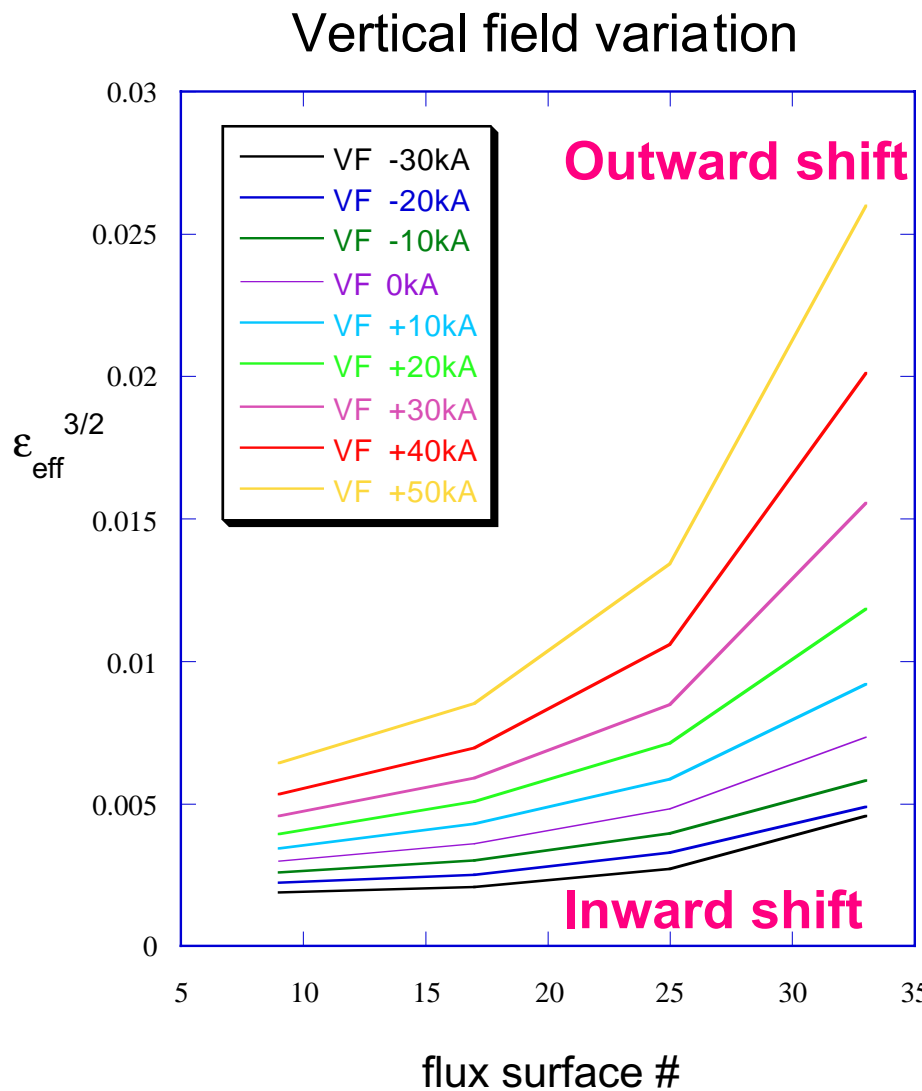


QPS FLEXIBILITY STUDIES

Flexibility is provided in QPS by 3 main coilsets.
By changing these coil currents, different configurations are possible.



Transport properties can be influenced either by varying the vertical or toroidal fields.



Conclusions

- QPS should be able to reach the plasma performance needed for its mission
- ISS95 scaling + ripple transport (0-D and 1-D) predict good performance
- Monte Carlo calculations of neoclassical component show that it is not a limiting feature
- The current 1108a4 configuration offers flexibility through the vertical, toroidal and modular coil currents
- A spectrum of transport analysis tools has been developed which - form a good basis for supporting a future experiment